iEnergy
REVIEW
https://doi.org/10.23919/IEN.2022.0007

Smart dielectric materials for next-generation electrical insulation

Xiaoyan Huang[1,†], Lu Han[1,†], Xiao Yang[2,†], Zhiwen Huang[1,†], Jun Hu[1], Qi Li[1] ✉ and Jinliang He[1] ✉

ABSTRACT

Smart dielectric materials with bioinspired and autonomous functions are expected to be designed and fabricated for next-generation electrical insulation. Similar to organisms, such dielectrics with self-adaptive, self-reporting, and self-healing capabilities can be employed to avoid, diagnose, and repair electrical damage to prevent catastrophic failure and even a blackout. Compared with traditional dielectrics, the utilization of smart materials not only increases the stability and durability of power apparatus but also reduces the costs of production and manufacturing. In this review, researches on self-adaptive, self-reporting, and self-healing dielectrics in the field of electrical insulation, and illuminating studies on smart polymers with autonomous functions in other fields are both introduced. The principles, methods, mechanisms, applications, and challenges of these materials are also briefly presented.

KEYWORDS

Bioinspired materials, next-generation dielectrics, self-adaptive materials, self-reporting materials, self-healing materials.

Traditional dielectric materials are designed and manufactured to be as robust as possible to prevent equipment failure and prolong the service life[1–5]. However, fatigue or degradation of dielectrics is ultimately inevitable, especially when operating under extreme conditions and harsh environments[6–9]. Nature serves as a source of inspiration for seeking innovative tactics to conquer this challenge. In nature, many animals and plants can survive in severe environments not merely due to their abilities to combat predators, resist injuries, and endure harsh environments. Most importantly, such organisms have evolved diverse behaviors and functions (such as anti-predator adaptation[10–13], nociception[14,15], and wound healing[16,17]) by natural selection to adjust to surroundings, perceive dangers, detect and repair injuries. Chameleons can change their skin colors by actively tuning a lattice of guanine nanocrystals in the dermis to blend in local environments to camouflage themselves from being detected by predators[18,19] (Figure 1(a)). Mammals may experience pain and discomfort when being subjected to an intense noxious stimulus due to the signal produced by nociceptors transferring along nerve fibers via the spinal cord to the brain, which prompts them to activate the body's defense system to avoid further harm[20,21] (Figure 1(b)). Roots and stems of plants, as well as skins and bones of animals, can autonomously heal by cell regeneration after being damaged, resulting in functional reconstruction and performance recovery[22,23] (Figure 1(c)). In the field of electrical insulation, we can similarly design and fabricate dielectric materials with bioinspired and autonomous functions to avoid, diagnose, and even repair electrical deterioration, which is conducive to improving the robustness of the dielectric materials and prolonging their service life.

The utilization of bionic smart dielectrics in equipment manufacturing is expected to spur the evolution of advanced power apparatus and even energy production, transmission, and utilization. With the rapid development of the global energy internet and ultra-high-voltage transmission technology, the demand for power apparatus with more reliable performance and longer lifetimes becomes greater and greater[24–26]. The stability and durability of electrical devices depend on the insulating materials[27,28], in which any defects or deteriorations extremely increase the risk of equipment failure and even a blackout[29]. The insulation problems become more and more complicated as the voltage level rises and the size of components shrinks[30–32]. For example, the unevenly distributed electric field withstood by insulating components in high voltage devices, such as cable terminals[33] and wall bushings[34], leads to particularly challenging problems with insulation design and equipment manufacture. Some power apparatus based on conventional techniques, such as terminals based on stress cones and bushings based on capacitor plates, hit a bottleneck in higher voltage levels[34–37]. In addition, a variety of factors, such as space charges[38], temperature[39], mechanical stress[40], ultraviolet[41], partial discharge[42], and even a tiny defect[43] may eventually result in a dielectric breakdown, making it exceedingly intractable to detect a latent insulation failure in numerous power apparatus[44–46]. Furthermore, solid insulation is unrecoverable[47], which means that any damage or degradation can permanently change its appearance and properties[48]. Therefore, deterioration accumulation in solid dielectrics continuously operating under a harsh environment will inevitably give rise to a catastrophic failure[49].

Developing biomimetic smart materials for the next-generation electrical insulation with self-adaptive, self-reporting, and self-healing capabilities is a novel solution to internal electric field grading, insulation defect detection, and electrical damage repairing in power apparatus. Self-adaptive dielectrics of which the electrical parameters are nonlinearly influenced by external field strength, exhibit an excellent ability to spatially grade the uneven electric field and rapidly release the intensive charges, avoiding insulation failure caused by the locally intensified field[50,51]. Self-reporting dielectrics can reveal a distinct variation in color, fluores-

[1]State Key Laboratory of Power System, Department of Electrical Engineering, Tsinghua University, Beijing 100084, China; [2]School of Electrical and Electronic Engineering, North China Electric Power University, Beijing 102206, China
† Xiaoyan Huang, Lu Han, Xiao Yang and Zhiwen Huang contributed equally to this work.
Address correspondence to Qi Li, qili1020@tsinghua.edu.cn; Jinliang He, hejl@tsinghua.edu.cn

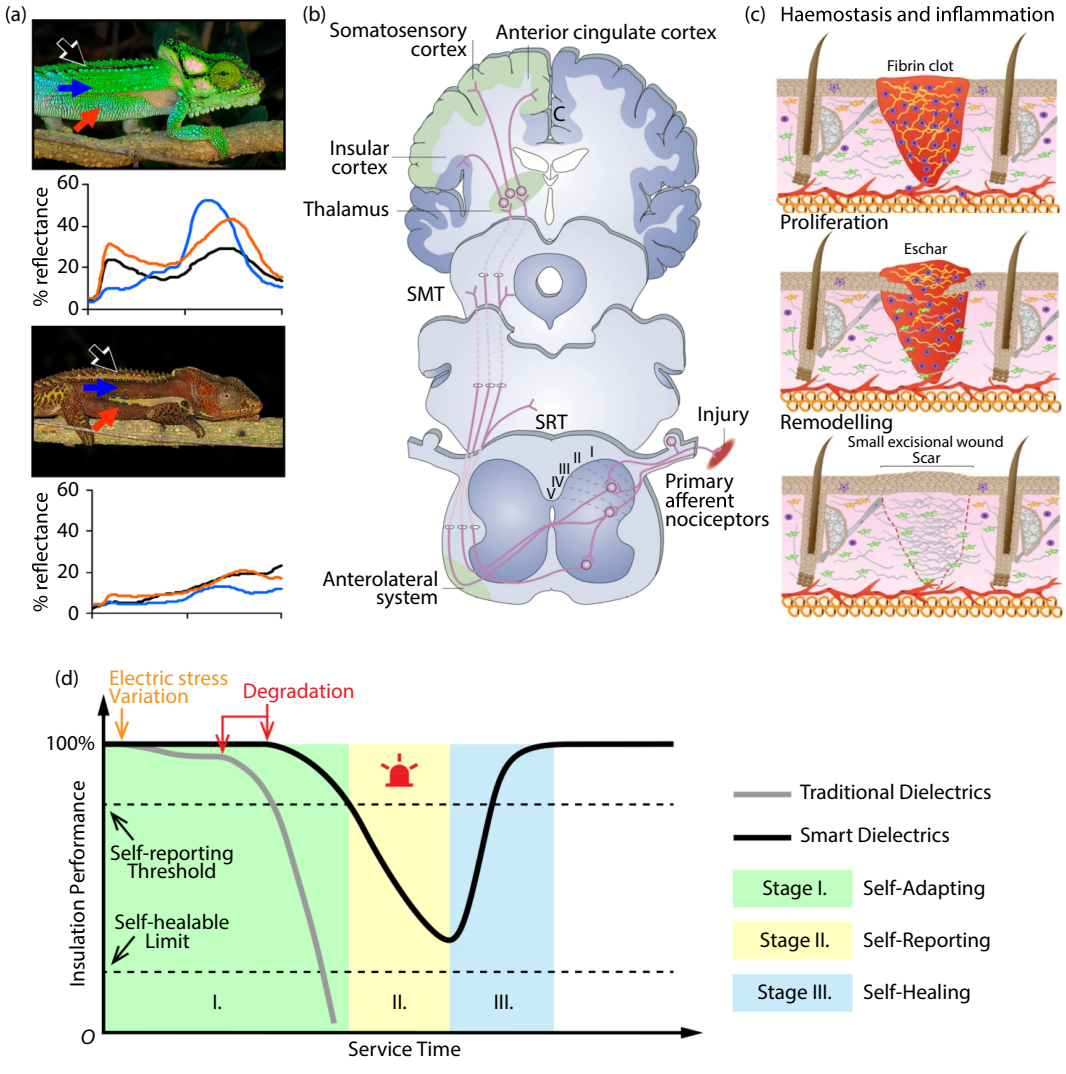

Fig. 1 Inspirations for designing smart dielectrics with biomimetic and autonomous functions. (**a**) Changes in the skin color and reflective spectrum of a chameleon (reprinted with permission from ref. [18], © 2008 Stuart-Fox and Moussalli). (**b**) Schematic of afferent pathways underlying the sensation of pain (reprinted with permission from ref. [15], © 2004 Nature Publishing Group). (**c**) Process of skin wound healing: haemostasis and inflammation, proliferation and remodeling (reprinted with permission from ref. [16], © 2019 Springer Nature). (**d**) Life cycle control of biomimetic smart materials for next-generation electrical insulation.

cence, or luminescence in response to internal performance degradation or external detrimental factors[52,53]. Therefore, the potential risk of catastrophic failure can be detected with the naked eye or optical monitoring facilities. Self-healing dielectrics can heal internal damage and recover the degraded properties to extend the lifetime of the materials[54–56]. By organically integrating the autonomous capabilities including self-adaptive, self-reporting, and self-healing functions into identical dielectrics, lifecycle control of insulating materials can be realized[57] (Figure 1(d)). At the stage of self-adapting, the electrical parameters of the smart dielectrics vary with environmental factors to maintain performance and avoid degradation. Once environmental degradation exceeds the endurance of the smart dielectrics, performance loss occurs, and the materials transfer to the self-reporting stage simultaneously. At the stage of self-reporting, unacceptable deterioration induces the smart dielectrics to display changes in appearance, and meanwhile, the self-healing process is triggered. At the stage of self-healing, the damage is repaired and the performance is recovered, and at the same time, the materials return to the self-adaptive stage. The above cycle can repeat a lot of times until the materials completely lost their autonomous functions. Compared with traditional dielectrics, the utilization of smart dielectrics not only increases the stability and prolongs the lifetime, but also reduces the costs of production and manufacturing.

In this review, researches on self-adaptive, self-reporting, and self-healing dielectrics in the field of electrical insulation, as well as instructive studies on smart polymers with bioinspired and autonomous functions in other fields, such as stimuli-chromic polymers for optical chemosensors, are both introduced. Principles, methods, mechanisms, applications, and challenges of smart materials are all presented in the following.

1 Self-adaptive dielectrics

1.1 Basic principles and mechanism of SADs

In nature, some smart creatures can self-adaptively take on different colors to merge into the background to escape predators. Similarly, smart dielectrics can adapt their electrical parameters to the spatial electric field to avoid insulation failure due to local intensified field strength[58], and we may call them self-adaptive dielectrics (SADs). Usually, SADs possess nonlinear conductivity $\sigma(E)$

or permittivity $\varepsilon(E)$ (or both) which increases rapidly with the local electric field when it exceeds a certain value[59,60], shown as Figure 2(a). This nonlinear electrical property endows SADs the virtue of self-adaptively grading electric field or releasing unwanted charges, whose mechanism can be generalized as: when SADs are working in moderated field strength, they behave just like common dielectrics with relatively low conductivity (~10^{-14} S/m) and permittivity (a little higher than the polymer matrix); and when local field strength tends to exceed the acceptable range, SADs exhibit much larger σ or ε as a response[50]. According to the law of current continuity shown as Eq. (1), larger σ or ε means lower field strength E under a continuous current density J, which can effectively suppress E to a safe value.

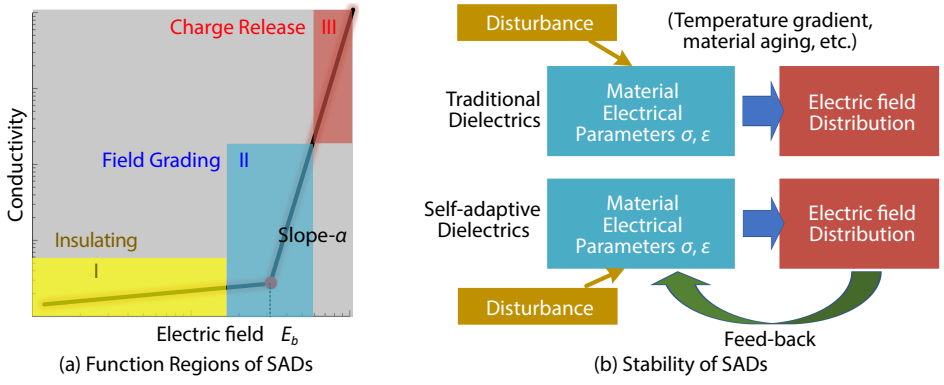

Fig. 2 Application mechanism of self-adaptive dielectrics. (**a**) Typical nonlinear $J(E)$ characteristics of SADs and their function regions. (**b**) Schematic diagram of the field grading mechanism of SADs.

$$J(E) = \sigma(E) \times E + \varepsilon(E) \times \mathrm{d}E/\mathrm{d}t \quad (1)$$

Furthermore, when overvoltage or discharging surges strike, SADs are expected to take on even larger σ to rapidly release the impulse energy to avoid damage to the equipment[61].

Simulations as well as experimental works have proved that the field grading or stress control performance of SADs is much better and more stable than traditional approaches[32,62,63] which mainly depend on the optimization of electrode structures of the apparatus. The advantage of field grading by SADs can be illustrated in Figure 2(b). In conventional approaches, material electrical property and electrode structure directly determine the spatial electric field distribution in power apparatus. Assuming the E-field as the control target, this approach is an open-loop control without any feed-back mechanism. In this case, the control performance is not satisfying and it is rather sensitive to parameter disturbance. For instance, little discrepancy of geometry of the field grading structure with fixed design can considerably affect the field grading effect[64], and temperature change or the material aging process can also lead to a much different E-field distribution with the expectation[65]. As a result, traditional approaches have encountered great challenges in the application of power apparatus with increasingly higher voltage level and more uneven electric field. On the contrary, field grading and stress control by SADs are typical closed-loop control. On one hand, the material parameters affect the electric field distribution; on the other hand, the electric field also feeds back to the material parameter which self-adaptively changes with it. In this case, an effective and stable field grading effect can be obtained by SADs regardless of the geometry discrepancy, different temperatures, or material aging.

For SADs, the most important parameters for their performances are the switching field E_b and the nonlinear coefficient α. E_b is defined as the switching point above which the material begins to exhibit a rocketing conductivity (permittivity)[66,67]. It should be adapted to specific applications as different power apparatus or electronic devices with different voltage levels has different requirements on the electric field. Thus, E_b of SADs is expected to be flexibly tuned according to practical cases, which may range from 0.1 to 5 kV/mm. How to choose an appropriate E_b for different applications is also an important issue, which is elaborated in the application part. In terms of the nonlinear coefficient α, it is the slope of $J(E)$ curve (in logarithmic coordinate) and reflects the degree of effect of electric field on material parameters. The greater the α is, the better the field grading performance will be. Ideal SADs are of an infinity α with vertical switching behavior. In practical cases, an α above 10 is high enough for field grading and stress control[58].

The above illustration shows that the key function of SADs is realized by a nonlinear conductivity or permittivity that rapidly switches with the electric field. For the former, many high-field conduction effects such as tuning or Schottky emission can result in a nonlinear conductivity[68]. However, these effects are not stable enough or may lead to a puncture of the insulation matrix. Furthermore, the nonlinearity due to these mechanisms is rather low and the switching field cannot be flexibly controlled. Therefore, most SADs with nonlinear conductivity are based on the mechanism of double-Schottky barrier whose height Φ_B is tuned by the localized states Q_i and applied electric field[69,70]. Under a relatively low electric field, the barrier height Φ_B only decreases a little with E, and the localized states Q_i even increases with E. The increased Q_i can stabilize the barrier and prevent Φ_B from fast decay. At this time, the conduction barrier is relatively high and it remains good insulation property. When the field strength is further higher, all the localized states are fulfilled and the stabilization effect of Q_i is of minor effect. This leads to a fast decrease of the barrier Φ_B and the current J flowing through the barrier significantly enhances, which results in an excellent nonlinear conducting. Additionally, the conduction relaxation effect can also lead to a nonlinear effective permittivity[71,72]. Thus, SADs based on this mechanism usually exhibit both nonlinear $\sigma(E)$ and $\varepsilon(E)$. In terms of SADs featured as nonlinear permittivity, materials with ferroelectric properties may exhibit a field-dependent $\varepsilon(E)$[73]. Nevertheless, both the coefficient and the maximum ε of these materials are not satisfying and can hardly be applied for field grading[67]. Above all, the nonlinear mechanism of most current SADs relies on the double-

Schottky barrier effect and their difference lies in various fabrication and connection approaches of the barrier, which shall be discussed in the material part.

1.2 Typical SADs and their nonlinear perfor-mances

For SADs that are applied in power apparatus or electronic devices, their major material system is the same with traditional polymer dielectrics for good compatibility, like crosslinked polyethylene (XLPE) for cables, silicone rubber for insulators, epoxy-paper for bushings, polydimethylsiloxane (PDMS) for device packaging, etc[59]. As polymer dielectrics themselves don't possess desired field-dependent electrical properties, doping of functional fillers is performed to endow them with nonlinear behaviors[50]. Thus, SADs are also called nonlinear composites. The most used functional (nonlinear conducting) fillers are SiC and ZnO microvaristors, which are raw materials for surge arrestors widely used in power systems[74,75]. Therefore, the microvaristor/polymer composites SADs are expected to possess excellent nonlinear $J(E)$ characteristics of arrestors. It has been elaborated that the nonlinear mechanism of SADs lies on the double Schottky barrier in the above part. There are also reports that the composites obtained by the graphene oxide or graphite nanosheets, and insulation matrix have nonlinear conductivity, which may come from the energy barrier formed on the surface of such fillers. The foundation of this kind of material is not enough comprehensive, and it has yet to be used in engineering practice[76,77]. For SADs with SiC fillers (denoted as SiC composites below, SADs with other fillers are the same), the Schottky barriers are formed over the interfaces between contacted SiC fillers[59], shown as Figure 3(a). In this case, the barrier height of the interfaces is relatively low, which means a relatively low α is also easily affected by filler concentrations and temperature. But for ZnO microvaristor fillers, the Schottky barrier lies on the grain boundary interior inside each filler particle, shown as Figure 3(b). Thus, each of the barrier heights is of high level and the nonlinear property of the composites is much more stable than SiC. Additionally, the switching field E_b of ZnO composites can be flexibly tuned according to specific requirements in the range of 0.3–2 kV/mm through controlling the grain size in the fillers, the filler diameter as well as the filler concentrations[78]. As a result, ZnO composites have attracted wide attention in the past decades, and their performance has been well studied[79,80]. However, the diameter of SiC particles is usually several micrometers but that of ZnO microvaristors is around tens of micrometers, which makes them easily precipitate in the polymer matrix and their combination with the matrix is rather loose[81]. Thus, for epoxy-based SADs and other applications that require good material mechanical properties, SiC fillers are preferred.

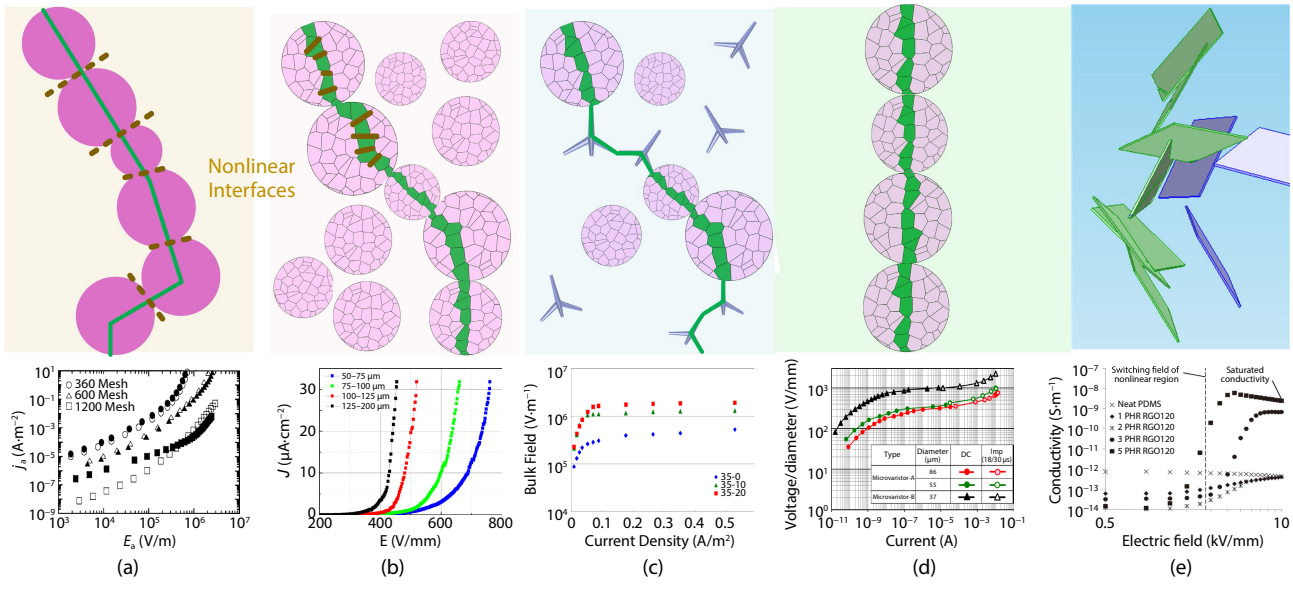

Fig. 3 Schematic diagram and $J(E)$ characteristics of SAD composites with (**a**) SiC (reprinted with permission from ref. [94], © 2001 American Institute of Physics). (**b**) ZnO microvaristor (reprinted with permission from ref. [78], © 2018 IEEE). (**c**) ZnO microvaristor and ZnO whisker (reprinted with permission from ref. [81], © 2012 IEEE). (**d**) Aligned ZnO whiskers (reprinted with permission from ref. [87], © 2014 IEEE). (**e**) GO nonlinear fillers (reprinted with permission from ref. [92], © 2012 WILEY-VCH Verlag GmbH & Co. KGaA, Weinheim).

For SADs, the thorough conduction paths of the functional fillers are usually required to guarantee stable nonlinear conducting behavior and charge release paths. As a result, filler concentration in the material is above 30 vol. %[82,83]. Heavy load of micro-sized fillers leads to poor mechanical property and large dielectric loss of the composites, which greatly limits the application of SADs in high voltage (HV) power apparatus which requires relatively high elasticity and low loss of the material. Researches have been carried out to reduce the concentration of the microvaristor fillers. One approach is employing secondary fillers to avoid heavy doping of functional fillers. For instance, SADs featured as a ternary system of ZnO microvaristor/carbon fiber/silicone rubber[51] have been investigated to enhance the mechanical property. On one hand, carbon fibers can replace parts of ZnO fillers to form the conduction paths, thus the concentration of those micro-sized particles can be reduced; on the other hand, carbon fibers can enhance the tensile strength of polymer materials. Similarly, low-dimensional semiconducting fillers including ZnO whiskers[81], carbon black[84], lamellar graphene[85], etc. have been investigated as secondary fillers for SADs, and improved mechanical property of the materials also have been reported, shown in Figure 3(c). Nevertheless, the usage of semiconducting fillers will result in an even greater loss of the composites. In this approach, the overall concentration of main and secondary fillers is still relatively high,

which prevents further modification of SADs and incorporation of other functional particles for multiple smart behaviors. Another approach is to align the functional fillers to form a straightforward conduction path through applying an AC electric field during solidification of the polymer matrix[86,87]. This method can reduce the filler concentration to below 10 vol. % (Figure 3(d)) but will bring further greater difficulty to the manufacturing of power apparatus or electronic devices with SADs. Thus, SADs obtained by this approach are only reported by laboratory research.

For better compatibility with polymer matrix as well as introducing further interface effects, nano-scaled functional fillers have also been investigated for SADs, in which nano ρ-SiC[88] and ZnO particles[89] are still the first choice. As conventional ZnO grain boundary structure can be hardly realized on nano-scaled particles, the double-Schottky barrier is constructed through the surface coating of Bi_2O_3, Co_2O_3 on ZnO nanofillers[90]. According to the percolation theory[91]. nano-scaled spherical particles can hardly form thorough conduction paths in composites. Also, research has proposed that besides the Schottky barrier effect, the hopping and tuning process in thin insulation polymer layer will also contribute to the nonlinear behavior of composites[88]. Therefore, the reported switching field E_b of the nanocomposites SADs are relatively high and their nonlinear coefficients are lower than these of traditional SADs. For nano-fillers with a high aspect ratio, such as wire-like, tube-like, or sheet-like ones, they can form conduction paths even under very low filler doping (around 10 vol. %). So far, SADs with the lowest filler concentration have been sheet-like graphene oxide (GO)/PDMS composites[92,93]. GO possesses excellent nonlinear conducting behavior as there are localized states at the interface between its conduction and insulation phase, which can form an energy band structure similar to the Schottky barrier. Then due to relatively high aspect ratio, a 3 vol. % concentration of GO can form stable conduction paths and the composites exhibit excellent nonlinear property with the coefficient of above 10, as shown in Figure 3(e). Besides the case of GO, low dimensional SiC and ZnO nanoparticles, such as SiC whisker or ZnO nanowire are also potentials for SADs with very light filler loading.

In summary, modern SADs are pursuing stable and high-level nonlinearity, flexible tuned switching field as well as the light load of nano-scaled fillers which has little effect on the original property of the polymer matrix. Advanced fabrication, modification, and assembling technology on low-dimensional particles are expected to endow SADs with further enhanced performances.

1.3 Power apparatus and devices based on SADs

Up to now, the conventional SADs with SiC, ZnO, and other semiconductors as fillers have drawn great attention from academia and industry. Numerous researches report the potential application of such materials in power systems, such as high voltage rotating machines, high voltage direct current (HVDC) spacers, and cable terminals, verified by experiments and simulations. Nonlinear materials have been applied earlier in the stator coil. Kelen et al. proposed a structure of SiC layer coating on the insulated conductor to suppress the surface partial discharges of stator coil ends in rotating machines[95]. Due to the nonlinear conductivity of SiC particle-loaded materials, the distribution of surface potential on the layer was almost straight. However, in the case of AC dielectric strength test, the test voltage frequently exceeded the limit of the SiC layer and results in a large current pass through, which may cause joule losses and temperature rise at the surface of SiC layer[96]. To solve this problem, a novel double-layer stress grading system for high voltage rotating machines was proposed by Umemoto et al., as shown in Figure 4[97]. The schematic of the typical insulation structure of the end-turn stress grading system is illustrated in Figure 4(a). In the novel system in Figure 4(b), SiC composites with higher conductivity were used as the first layer to cover the end of conductive slot, while SiC composites with lower conductivity were the second layer to cover the end of the first layer for heating suppression. The way to obtain such materials with different potential gradients was to control the particle size of SiC as fillers. According to the conductivity test results, samples with larger particle sizes showed a higher conductivity and the composites with an average particle size of 20 and 11.5 μm were chosen for the first and second layers, respectively. The distributions of surface potential and time-averaged power dissipations

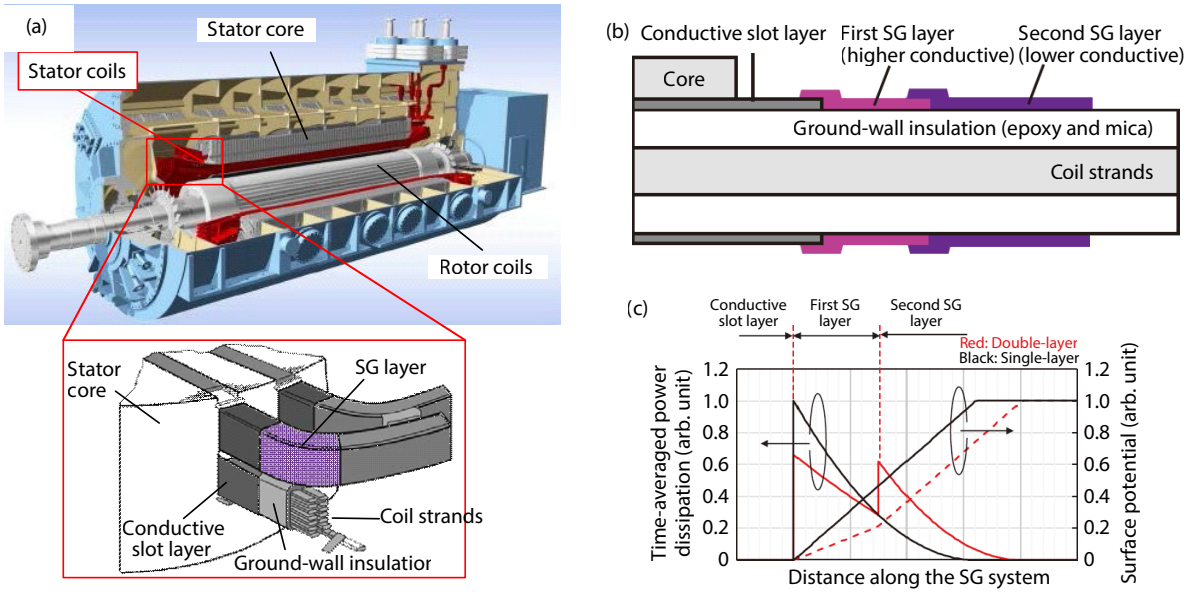

Fig. 4 Examples of SADs used in motor coils. (**a**) Schematic of a turbogenerator and typical insulation structure of the end-turn stress grading system. (**b**) Cross-section of the double-layer stress grading system. (**c**) Distributions of surface potential and time-averaged power dissipations along the stress grading systems. Reproduced with permission from ref. [97], © 2020 IEEE.

along the single-layer and double-layer stress grading system calculated are shown in Figure 4(c). The effectiveness of the system was successfully confirmed by both simulation and experiment, which showed more than 15% higher flashover voltage and better heat suppression than the conventional single-layer ones.

Another example of application is to uniformize the locally intensified electric field of polymeric outdoor insulators. Because of the rod-like structure, the nonuniform distribution of electric field along the insulator is a fundamental problem. Yang et al. presented a design in which a SADs layer was applied near the terminals to achieve a homogenous electric distribution, shown in Figure 5(a)[50]. After the optimization simulation of geometry and parameters of the SADs layer, they prepared a 220 kV prototype and electric field distribution measurements were performed by an optical electric field sensor at 10 reference points. The simulated electric field distribution on insulators with the SADs layer in Figure 5(b) had a significant decrease at the end of the insulator string than the traditional insulator. As shown in Figure 5(c), the maximum electric field and nonuniformity of electric field distribution of the traditional insulator are greater than that of the insulator with a nonlinear layer.

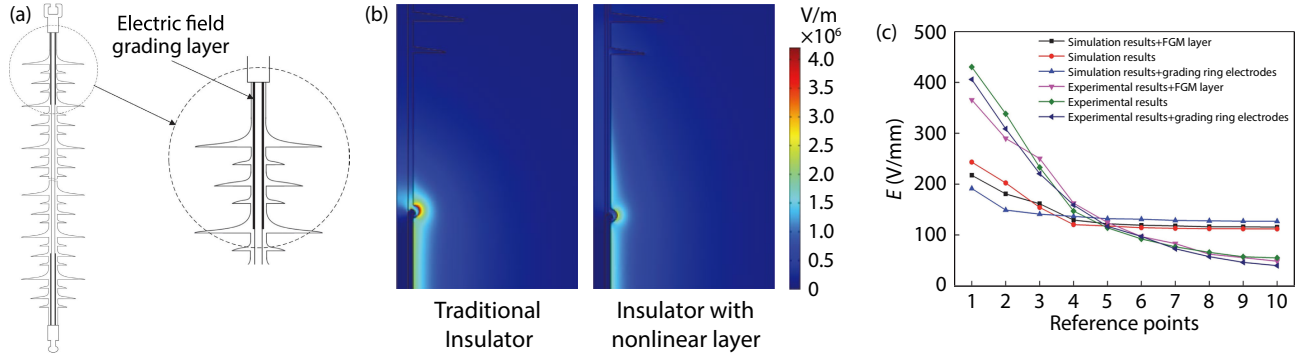

Fig. 5 Application of SADs in polymeric outdoor insulators. (**a**) Schematic of insulators with nonlinear materials. (**b**) Electric field distribution of traditional and novel insulators. (**c**) Electric field distributions from simulations and experiments at 10 reference points along the 220 kV insulator. Reproduced with permission from ref. [50], © 2018 IEEE.

The major concern of HVDC spacers is the surface discharge during operating, which can significantly affect the stability of the GIS system. Li et al. analyzed the charge transport and control strategy of the HVDC spacers and put forward a novel model based on the materials with nonlinear conductivity to release the surface charge accumulation, as shown in Figure 6[98–100]. The charge adaptive spacer (CACS) was shaped like a bowl, which was composed of the insulation region and the charge adaptive control region. This design allowed the CACS to meet the requirements of the longitudinal mechanic force, and more crucially, the normal component of the electric field may be centered on the spacer's sidewall near the ground enclosure, as shown in Figure 6(a). CACS with different properties were optimized by changing the ratio of Al_2O_3, SiC, and epoxy resin. To prove the effect of nonlinear material on limiting surface charge, the regular spacer (RS), novel shaped spacer (NSS), and charge adaptive spacer (CACS) was compared under AC and DC surface flashover tests. The AC surface flashover voltage of NSS and CACS range from 200 to 225 kV, which were higher than RS with a breakdown value ranging from 160 to 180 kV, as shown in Figure 6(b). The dispersity of the test results of CACS was lower than RS and NSS and this may indicate that nonlinear materials have a more stable effect on limiting charge aggregation. The test results of DC surface flashover test, shown in Figure 6(c), revealed that the values for different samples show a small difference. The flashover value of RS was almost the same as NSS and CACS, which range from −270 to −300 kV and the mean breakdown values of them were all in the range of −285 to −290 kV. However, under step voltage, the surface flashover value of CACS, ranging from −280 to −290 kV, was significantly higher than RS and NSS with values mainly lying from −270 to −280 kV. In addition, the model spacer based on nonlinear materials had good competitiveness in the test of thermal performance and mechanical performance according to their report.

For the applications in power delivery equipment, such as cable accessories, some institutions have manufactured prototypes that

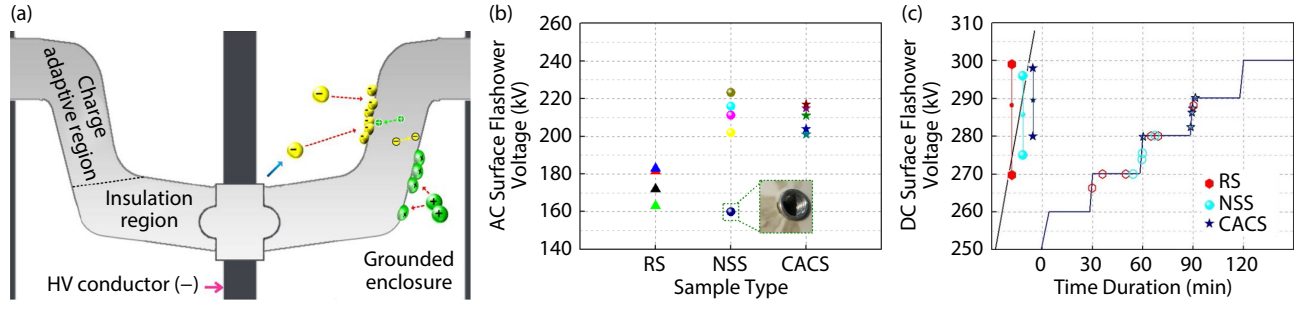

Fig. 6 A novel HVDC spacer based on SADs. (**a**) The structure of the spacer and the space charge migration (reprinted with permission from ref. [98], © 2018 IEEE). (**b**) AC surface flashover test results of experimental samples (reprinted with permission from ref. [99], © 2018 IEEE). (**c**) DC surface flashover test results of experimental samples (reprinted with permission from ref. [99], © 2018 IEEE).

can be used to test. Asea Brown Boveri (ABB) has developed the prototype of a cold shrink 84 kV cable termination with ZnO microvaristors/SiR composites[101]. And it is reported that the prototype successfully passed all the tests including discharge tests, AC withstand tests, and lighting performed on a 72 kV cable. A dry outdoor vertical 145 kV cable terminal based on nonlinear material was also developed successfully[102]. At present, cable accessories with higher voltage based on nonlinear materials are not yet implemented, but plenty of simulations and designs have been carried out by researchers[58,102].

The operation reliability of high voltage bushing is a key problem in power transmission projects. With a cylindrical structure in the radial direction and a "plug-in" structure in the axial direction, the concentration of electric field may cause the discharge or even breakdown of the insulation. In general, the method to avoid the issue is to build a multi-capacitor layer structure, which also makes its production process complex and quality control difficult. For this widespread problem, it is very effective to create a grading system by nonlinear materials. Zhao et al. designed an only three-layer adaptive bushing based on nonlinear materials[34]. The structure diagram is shown in Figure 7(a)[34]. The field grading layer used the conventional nonlinear composites material with a low nonlinear coefficient and high threshold electric field for the field grading in the radial distribution of electric field, while the electrode extended layer used ZnO microvaristors particle-loaded one with a high nonlinear coefficient and low threshold electric field for the suppression discharge at the edge of the flange. The leakage current limiting layer was composed of general insulation materials, such as epoxy and linked polyethylene, to reduce the loss of heating. The size and material parameters of each layer were optimized separately by finite element simulation and the radial electric field distribution of the capacitance-graded bushing and the adaptive bushing under various temperature fields are shown in Figure 7(b)[34]. For the capacitive bushing, the radial electric field distribution was reversed under high-temperature field, which can be attributed to the variation conductivity of the insulation material in the condenser core. The electric field grading method of this bushing completely depends on the multi-capacitance structure, which means that once the internal material properties changes, the maximum electric field will continuously grow. As for the adaptive bushing, the grading system composed of nonlinear materials at the field grading layer introduced feedback to the parameters of materials to adapt the temperature field, and the maximum electric field was limited to about 50% with a value of 4 kV/mm. Another essential problem was the weak point at the flange with strong vertical electric field. The condenser core of multi-capacitance system could shield the flange but also triggers an electric concentration at the end of the last condenser core with a simulated value of 8.39 kV/mm, as seen in Figure 7(c)[34]. The electrode extended layer in the novel structure used a class of highly nonlinear material to establish an equivalent electrode with local high conductivity near the edge of the flange and the maximum electric field in the whole insulation decreased to 4.58 kV/mm.

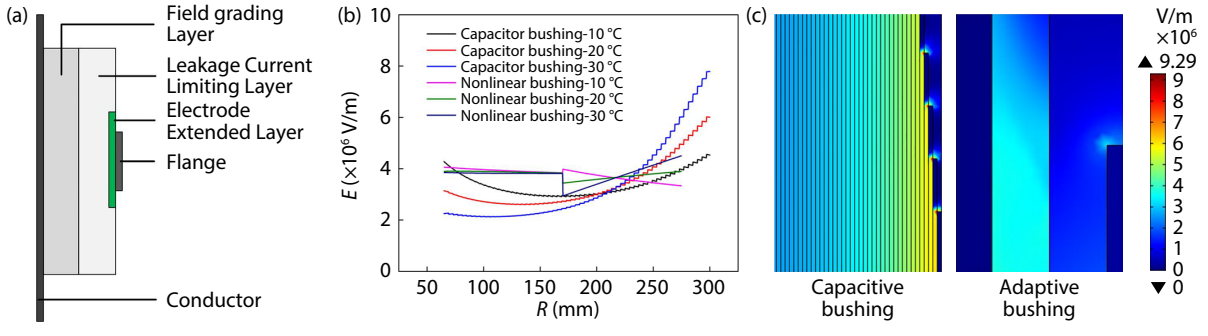

Fig. 7 Design of adaptive bushing based on SADs. (**a**) Structural diagram of adaptive bushing. (**b**) Radial electric field distribution under various temperature differences. (**c**) Electric field distribution of the capacitive bushing and adaptive bushing. Reprinted with permission from ref. [34], © 2021 The Authors.

For application in electronics, Wang et al. first proposed the idea of using composites with nonlinear conductivity as novel packaging materials of power electronic module to achieve a homogeneous distribution of electric field[103]. They added a ferroelectric filler barium titanite to a silicon-based gel to form a composite gel with nonlinear conductivity. Using this composite gel in a power electronics module through finite element simulation, the electric field level near the metalized edge of the substrate was significantly reduced. However, one of the methods to adjust the conductivity of composites gel was to change the filler volume, which may increase the viscosity of the gel and could not be used. Based on the ZnO microvaristors particle-loaded nonlinear composites with a lower threshold electric field and higher nonlinear coefficient at the same filler volume, Donzel of ABB proposed the design of ZnO microvaristors/polyimide composites as a layer coating on the Aluminium nitride (AlN) substrate of insulated gate bipolar transistor (IGBT)[104]. To achieve the best effect of grading electric field, they controlled the sintering temperature and dwell time of the ZnO microvaristors to adjust the grading effect and the composites with a relative permittivity of 12 and a nonlinear coefficient of 12 were chosen. By means of finite element simulations, they established a model of the novel system to evaluate the distribution of electric field. The simulation model without an extra coating layer showed a maximum electric field inside the silicone gel of 260 kV/mm, which may result in failure of partial discharge test. While for the model with a coating layer, an efficient electric field reduction was obtained by superior grading performance of nonlinear materials. The electric field at the critical triple point was significantly reduced and the maximum electric field values were as low as 7 and 6 kV/mm at the protrusion and the layer interface, respectively.

1.4 Outlook for SADs

New materials have been widely acknowledged as one of the biggest opportunities for the next generation of electric equipment, coexisting with challenges. We believe deeper research of SADs would benefit the design and manufacture of various power equipment. Future SADs, as intelligent materials, can adapt to

various voltage levels in different power equipment, so as to uniformize electric field distribution, improve insulation performance and reduce the size of equipment. Another market with huge potential for SADs is the application in electronics. With the development of electronics towards high integration and power, electronics instruments suffer from local high electric field, overshoot voltage, and electrostatic discharge by the sharp reduction in production size and ever-increasing power density. Just like the creatures in nature adapting to the environment, we would like to see SADs available for all kinds of problems caused by electrical overstress.

2 Self-reporting dielectrics

Self-reporting materials[57,105], also known as self-sensing materials[106,107], are smart polymers that can report information on internal performance and external surroundings by changing physical or chemical properties in response to extrinsic stimuli such as light[108], temperature[109], mechanical stress[110], electrical potential[111], pH[112], ions[113], biological ligands[114], etc. Numerous natural events serve as inspiration for fabricating self-reporting materials. When an animal's skin is injured, for example, blood flow and pain perception are presented, which can help the animal sense and escape danger swiftly[105]. In recent years, self-reporting materials have mostly been used to detect mechanical stress[115], microcracks[116], and metal corrosion[117]. However, to the best of our knowledge, the application of self-reporting insulating materials in the electricity sector has not been thoroughly reported. Solid insulation is unrecoverable, therefore the accumulation of damage and deterioration raises the probability of electrical failure, especially when electrical equipment is used for an extended period of time in a harsh environment, such as UV irradiation, overheating, acid rain, stress concentration. In addition, under extremely high voltage and strong electric field, even a tiny insulation defect anywhere may lead to a breakdown with no apparent indication or warning. As a result, the unpredictability of insulation failure makes early detection and prevention exceedingly challenging. In contrast to monitoring and measuring by external equipment, programming dielectrics with bioinspired and autonomous capabilities to deliver a visible alert to potential risks in solid insulation is a more facile and efficient approach to overcoming the obstacles mentioned above. These biomimetic dielectric materials with autonomous forewarning abilities might as well be referred to as self-reporting dielectrics (SRDs). If the technology of synthesis and utility of SRDs matures, the damage and deterioration in solid insulation can be detected by the naked eye or optical monitoring devices conveniently. Furthermore, the security and stability of transmission lines and electrical equipment will be heavily promoted.

In the field of basic research in materials science, stimuli-response materials and sensing materials, which are comparable to the notion of self-reporting materials, are more generally focused and intensively explored[118,119]. Up to now, a large number of smart materials have been developed to sense and detect a variety of physical quantities, chemical surroundings, or biological targets. Stimuli-chromism, which involves photochromism[120], thermochromism[121], mechano-chromism[122], hydrochromism[123], solvatochromism[124], electrochromism[125], and so on, is the most typical response of these materials undergoing activation by external stimuli. Such stimulants can also trigger some of them to emit fluorescence[126,127] or luminescence[128,129]. A wide range of studies have focused on this type of smart material owing to its broad variety of advanced applications in aerospace[130], automotive[131], civil engineering[132], electrical engineering[133], microelectronics[134], printing[135], chemosensors[136], bioimaging[137], drug delivery[138], etc. These outstanding researches have the potential to motivate the development and application of SRDs in electrical insulation. So far, plenty of comprehensive reviews have been published concerning bioinspired materials[139–141], stimuli-responsive materials[118,142,143], sensing materials[119], and self-reporting materials[105,116,117,144]. Concepts, syntheses, mechanisms, applications, and challenges are introduced in detail. In this section, the fundamental concepts and essential principles of several types of extensively investigated and widely implemented smart polymers that contribute to the fabrication and utility of SRDs are induced and presented.

Self-reporting materials based on photochromic compounds, conjugated polymers, and microencapsulated systems are introduced in the following. Photochromic compounds are organic small molecules isomerizing between two chemical structures with different physical or chemical characteristics in response to light irradiation[118]. By physically or chemically incorporating them into polymer matrices, a great number of self-reporting materials with the ability to respond to various stimuli can be manufactured. Conjugated polymers such as polydiacetylenes (PDAs) possess fascinating and valuable optical and electronic properties due to their unique backbone formed by alternating single and double bonds[145]. Different degrees of backbone distortion induced by interactions between side chains and external stimuli cause varied macroscope colors of PDAs. A wide range of highly visualized, flexible, and selective self-reporting materials are fabricated by modification methods based on decorating diacetylene monomers and synthesizing composite materials[146]. Microencapsulated systems are independent material systems composed of indicator solutions for visualizing the damage inside bulk polymers or on their surfaces, as well as encapsulating containers for isolating indicators from their surrounding environment[144]. Attributed to the existence of encapsulating containers, the detrimental interactions between microencapsulated indicators and polymeric matrices are eliminated. This type of material is commonly used to detect polymer damage or fatigue, along with metal corrosion.

2.1 Self-reporting materials based on photo-chromic compounds

Photochromic compounds, such as spiropyran, spirooxazine, azobenzene, diarylethenes, and their derivatives, undergo photo-induced isomerization leading to a change in physical and chemical properties[118]. These compounds also display a variation in visible light absorption or fluorescence emission in response to other stimuli, including polarity, pH, temperature, etc., owing to the high chemical activity of specific groups or bonds[147–150]. Spiropyran (SP) and its derivatives[151] are the most extensively explored photochromic compounds, which consist of indoline and chromene moieties. In the inactivated state, the planes of the two moieties are orthogonal, the chromene moiety presents a ring-closed form, and the SP molecule is hydrophobic, nonpolar, and colorless. The ultraviolet (UV) light-induced bond cleavage of the spiro C–O takes place, along with the molecule isomerizing to a hydrophilic, polar, and colored merocyanine (MC) form with a conjugated planar zwitterionic structure. And the ring-opened MC molecule reverses to the ring-closed SP form upon visible light irradiation or heat (Figure 8). Spirooxazine and its derivatives[152] have a structure and a stimuli-chromic mechanism similar to spiropyran. They display a good response towards various external stimuli and

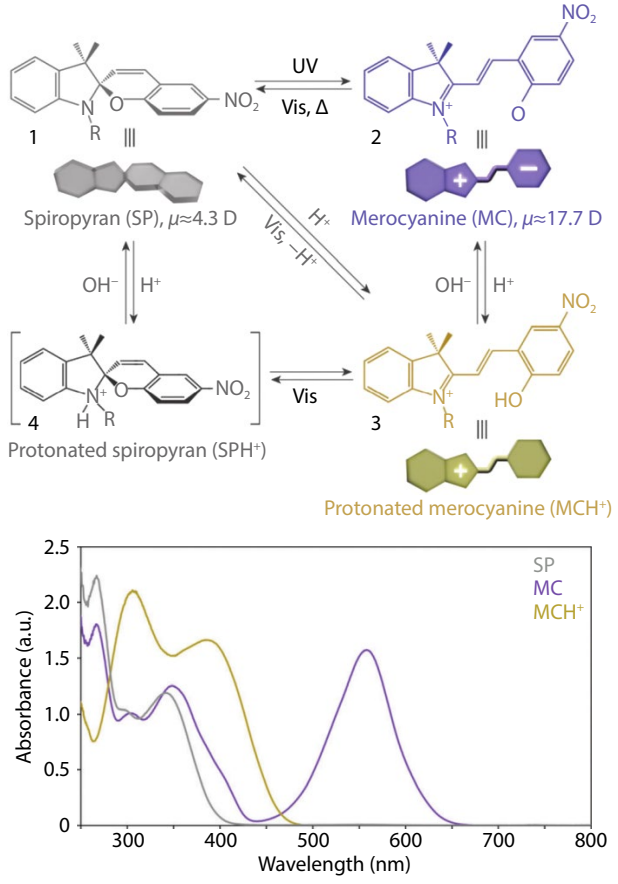

Fig. 8 Photochromism and acidochromism of spiropyran. (**a**) Reversible transformations between the four states: spiropyran (SP) 1, merocyanine (MC) 2, protonated merocyanine (MCH^+) 3, and protonated spiropyran (SPH^+) 4. (**b**) UV–Vis spectra of the parent spiropyran before (gray) and after (purple) UV irradiation, and after the addition of HCl (yellow). Reprinted with permission from ref. [151], © 2014 The Royal Society of Chemistry.

show a higher fatigue-resistance and a longer lifetime compared with spiropyran. The azo group of azobenzene and its derivatives[153] undergoes trans-cis isomerization when exposed to UV/visible light irradiation or heat. The variation in chemical structure not only induces a color change in azobenzene but also affects the physicochemical characteristics of its surrounding medium significantly. Dithienylethene[154] is a kind of diarylethene derivative that is widely used. A reversible cycloaddition reaction occurs under alternating UV and visible light irradiation, along with a photochromic phenomenon. Photoswitchable conductive materials containing dithienylethenes have the potential to be practically implemented in the commercial sector. Activated dithienylenthene possesses stronger visible light absorption and higher conductivity than its ring-opened form. By physically and chemically incorporating photochromic compounds into polymeric matrices such as doping[155], copolymerization[156], crosslinking[157], and grafting[158], a wide range of self-reporting materials with a variety of stimuli-responsive behaviors can be manufactured.

Photochromism is the most fundamental characteristic of photochromic compounds. The chromophore that is sensitive to the surrounding properties is required to be protected from destruction in the process of preparing. An improvement in photoswitchability, reversibility, photostability, and photofatigue resistance is expected to be achieved by the rational design and synthesis of photo-responsive polymers[118]. Schenderlein et al.[159] chemically incorporated a terpolymer consisting of SP moieties, benzophenone groups, and dimethylacrylamide units onto planar silicon and glass surfaces by UV irradiation and subsequently synthesized surface-attached, light-switchable polymer networks. The UV/vis absorption peak and the maximum wavelengths (λ_{max}) of the photochromic surface varied corresponding to the intensity and duration of UV illumination. As a result, the intensity of unknown UV irradiation could be deduced by the color or visible light absorption spectrum of the surface.

Plenty of polymers undergo mechanical stress such as tension, compression, and shear in engineering applications. Therefore, self-sensing of fatigue, degradation, and failure in materials conduces to the robustness and stability of mechanical systems. Davis et al. proposed a self-reporting method for sensing force-induced deterioration and failure of polymers[52]. In this method, SP as a mechanophore was incorporated into polymers, and both moieties of the molecule were individually connected to a polymeric chain. The force-induced deformation of polymeric matrices intensified the tensile stress of SP molecules so that a bond cleavage of spiro C–O took place, resulting in the colorless molecules isomerizing to the colored MC form. Subsequently, a color shift in the site of deformation or deterioration was observed, and the degree of it deepened as the stress on the matrices was enhanced until a fracture of the material occurred (Figure 9(a)). Spiropyran mechanophores have so far been utilized in all kinds of glassy (such as poly (methyl methacrylate)[160], polystyrene[161], polycaprolactone[162], etc.) and rubbery (polymethacrylate[52], polyurethane[163], polydimethylsiloxane[157], etc.) polymeric matrices successfully. In addition, Kosuge et al. synthesized a novel force-induced self-reporting polymer by employing diarylbibenzofuranone (DABBF) as a mechanophore and investigated its mechanochromic characteristics systematically[164]. The central C–C bond rupture of the DABBF group upon mechanical force led to the formation of stable blue radicals, and thus a color variation of the material from light yellow to blue occurred. They also fabricated a multicolor mechanochromic polymer/silica composite by using the two types of mechanophore mentioned above, which exhibited multiple color states in response to different intensities of applied external stimuli (Figure 9(b))[165].

The electrochromic materials are manufactured by incorporating the photochromic compounds into electroactive matrices including conductive polymers, gold nanoparticles, and electrolyte solutions. Zhu et al. explored the electrochromic behaviors of two types of oxazine derivatives in both solution and indium tin oxide (ITO) devices[166]. When the chromophore was activated by electric stimuli, the opening reaction of the oxazine took place, leading to a color change from yellow to blue. They measured as well the UV/vis absorption spectrum of the material as the applied electrical potential varied in the range of 0–2.1 V and revealed that the higher the voltage applied, the stronger the absorption intensity of visible light and the more obvious the color variation was (Figure 10(a)). Based on the characteristics mentioned above, the material has the potential to be used to detect the magnitude of an unknown voltage applied to it.

The photochromic property of spiropyran is affected by its surrounding media. To be precise, the interactions between the photo-triggered zwitterionic MC molecules and the solvents or media impact the polarity of the molecules themselves, resulting in a variety of colors being presented. This phenomenon is referred to as photoswitchable solvatochromism of spiropyran. Rosario et al. studied the solvatochromism of a spiropyran-modified surface of glass substrates in different solvents with various polarities[167]. The

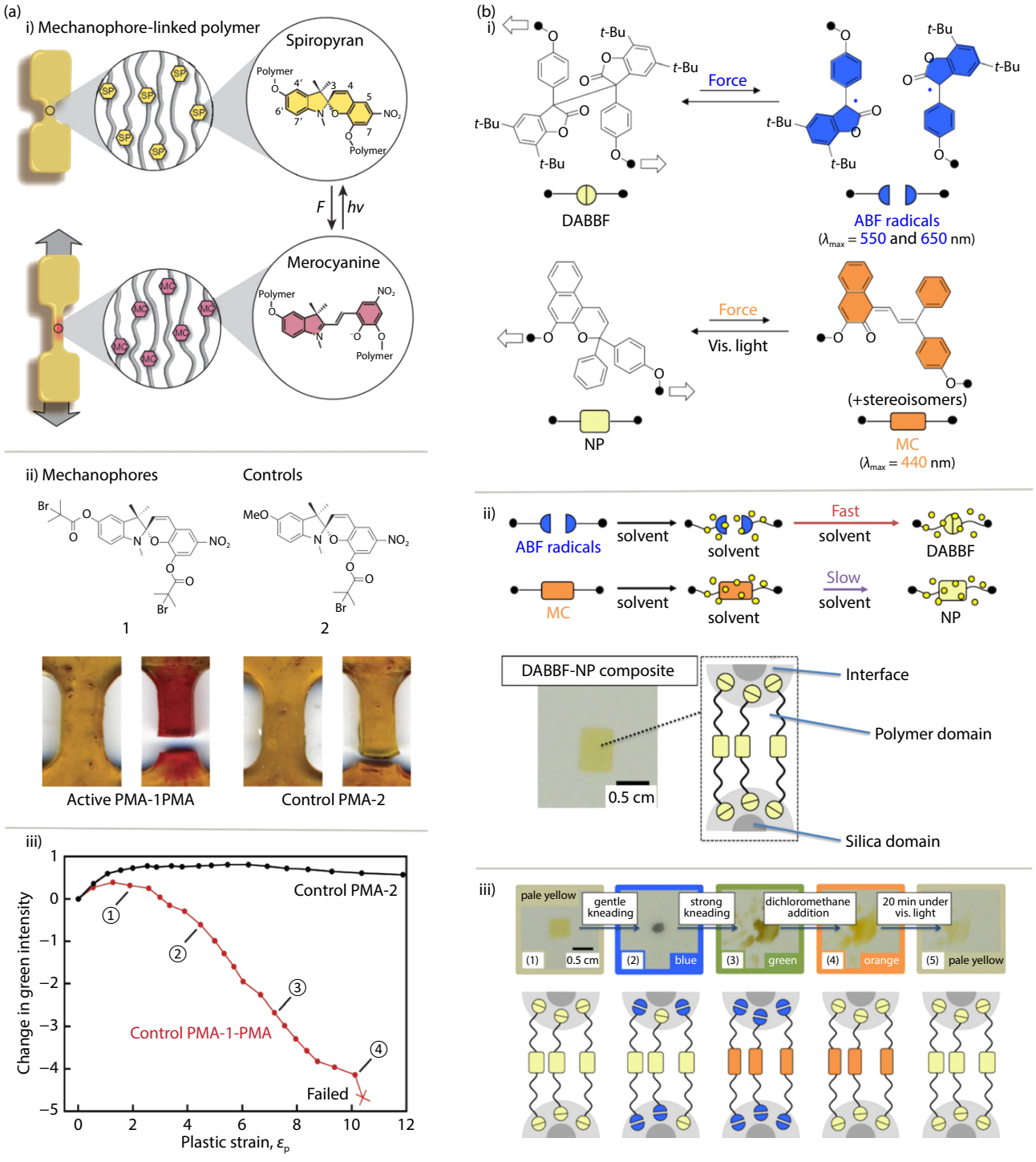

Fig. 9 Force-induced self-reporting materials. (**a**) Spiropyran as a mechanophore. (i) Schematic diagram of a mechanophore-linked PMA "dog bone" specimen and its mechanochromic behaviour. (ii) Distinct effects of tensile loading on the active PMA-1-PMA and monofunctional PMA-2 specimens. (iii) Accumulation of plastic (unrecovered) strain and relative change in green intensity for PMA-1-PMA and PMA-2 samples after each loading cycle in a fatigue test. Reproduced with permission from ref. [52], © 2009 Macmillan Publishers Limited. (**b**) Multicolor mechanochromism of a polymer/silica composite with dual distinct mechanophores. (i) Chemical structures of two mechanophores and their activated states. (ii) Illustration of the two mechanophores' locations in the sample and their reversible mechanochromic behaviours. (iii) Optical photographs and plausible illustrations showing mechanophores' activation states in the pristine, gently kneaded, strongly kneaded, and dichloromethane–added samples, and the sample left under visible light for 20 min after dichloromethane addition. Reproduced with permission from ref. [165], © 2019 American Chemical Society.

UV/vis absorption and fluorescence emission λ_{max} of the surface on which the SP chromophore was covalently incorporated exhibited a hypsochromic shift as the polarity of the solvents was enhanced. In high polarity solvents containing hydrogen bonds, the hydrogen bonding and dipole-dipole interactions between the zwitterionic MCs and the solvents stabilized the ring-opened molecules, and therefore a negative photochromic phenomenon was observed. Based on the aforementioned mechanism, self- report-

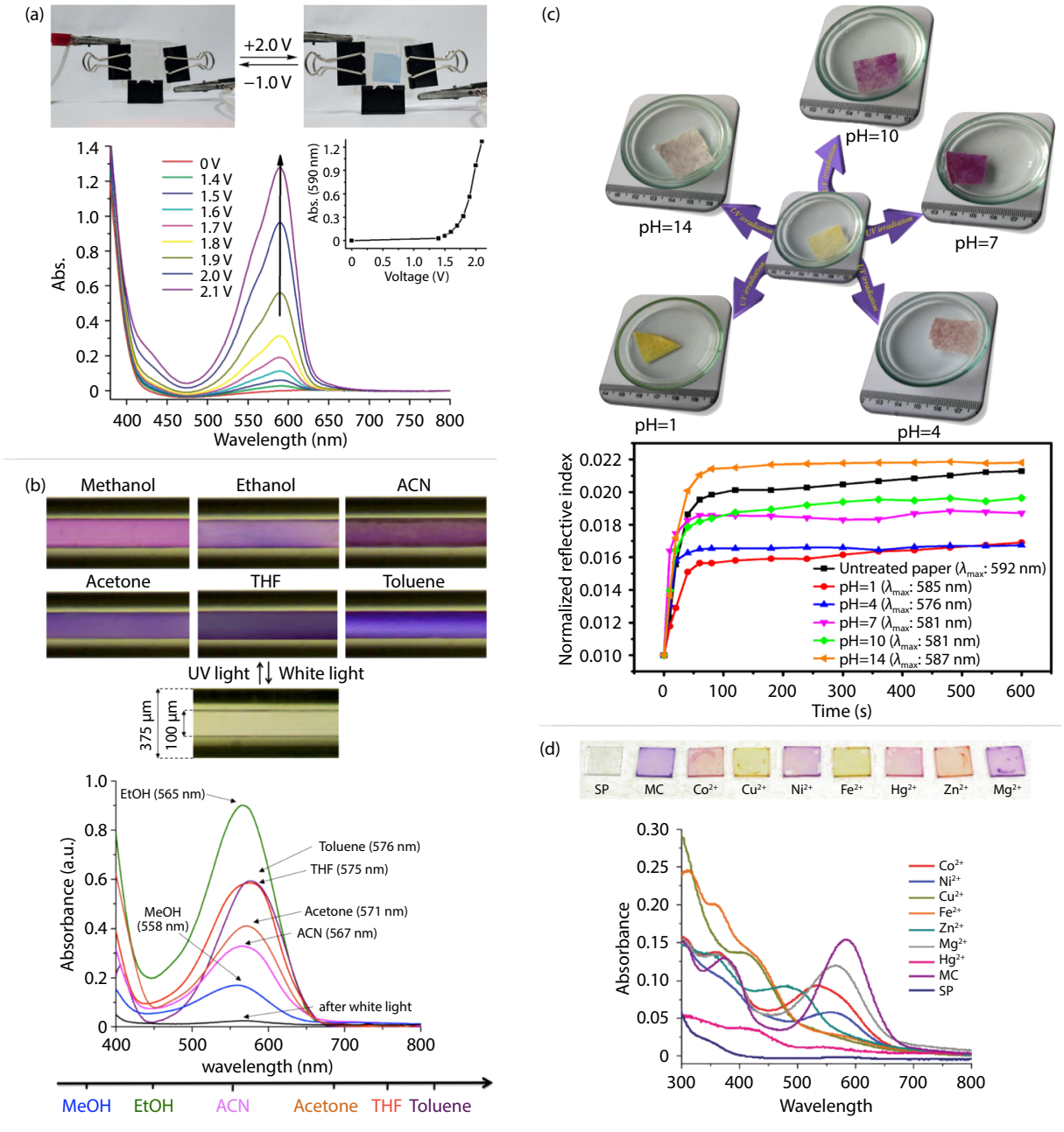

Fig. 10 Some stimuli-chromic phenomena of smart materials based on photochromic compounds. (**a**) Real objects illustration of the electrochromism for an oxazine derivative and its UV/Vis absorption spectra in THF (reprinted with permission from ref. [166], © 2014 WILEY-VCH Verlag GmbH & Co. KGaA, Weinheim). (**b**) Pictures of the solvatochromic microcapillary when irradiated with UV light while different solvents are passed through the microcapillary in continuous flow and after irradiation with white light (reprinted with permission from ref. [168], © 2013 American Chemical Society). (**c**) Color changes of the prepared stimuli-responsive paper in various pHs under UV irradiation at 365 nm, and normalized reflective index at the corresponding λ_{max} for the untreated paper and the treated ones in different pHs (reprinted with permission from ref. [169], © 2018 Elsevier). (**d**) UV-Vis spectra in the presence of different metal ions of reversible colorimetric ion sensors based on surface-initiated polymerization of photochromic polymers (reprinted with permission from ref. [170], © 2008 The Royal Society of Chemistry).

ing materials with the ability to sense the polarity of their surroundings and identify a variety of organic solvents can be designed and synthesized. Florea et al. prepared a sensing material that can detect solvents with different polarities by incorporating SP functionalized polymer brushes into fused silica microcapillaries[168]. The SP chromophores that were activated to MC isomers by UV irradiation in advance were influenced by solvents with diverse polarities flowing through the microcapillaries continuously, and thus displayed a series of optical and spectral responses correspondingly (Figure 10(b)). Upon further analysis of the color and spectrum, the type of unknown solvent could be established facilely.

The acidochromic mechanism can be interpreted that the ring-opened MC isomer of spiropyran exists in the form of yellow protonated MCH^+ in the acidic or protonic media but recovers to the purple MC form in basic or aprotic surroundings (Figure 8). In order to maintain the chemical activity of the acidochromophore in nonpolar solvents, spiropyran is required to be triggered by UV light to avoid it isomerizing back to the ring-closed form. Abdollahi et al. prepared a novel photoswitchable pH sensing material by chemically incorporating latex particles containing spiropyran into cellulose[169]. The material was able to rapidly respond to

solvents with varying pH levels by exhibiting a variety of colors (Figure 10(c)).

The zwitterionic MC isomer can coordinate with various ions and hence presents multiple colors, which is known as the ionochromic property of spiropyran. Its electron-rich phenolate moiety is facile to incorporate with cations, while the electron-deficient indolium ring is sensible to anions. Fries et al. obtained a photoswitchable ionochromic material by covalently binding the copolymer of spiropyran methacrylate derivative (SPMA) and methyl methacrylate (MMA) onto the surface of a glass substrate[170]. The surface showed a specific optical and spectral response to several divalent metal cations (Figure 10(d)). In addition, Shiraishi et al. demonstrated that nitrospiropyran could also detect the cyanide ion (CN^-) in aqueous[171].

2.2 Self-reporting materials based on conjugated polymers

Conjugated polymers, such as polydiacetylene (PDA), polythiophene, polypyrrole, etc., are organic macro-molecules with a backbone consisting of alternating single bonds and double bonds. Their π-electron delocalization formed by the overlap p-orbitals results in attractive optical and electronic properties[145]. PDA with excellent stimuli-responsive characteristics has enormous potential to endow the self-reporting ability to polymeric dielectrics. It shows an apparent color change in response to a wide range of physical, chemical, and biological stimuli, such as temperature, mechanical stress, current, organic solvent, ions, biomolecules, etc. When PDA is excited by external stimuli, the conformation distortion of its backbone leads to an increase in the freedom of motion and randomness of the side chains. Less coplanar side chains and shorter p-conjugation length causes that the UV/vis absorption peak undergoes a hypsochromic shift from 650 to 550 nm, which means that the material displays a distinct color change from blue to red[172].

Thermochromism is the most fundamental stimuli-responsive property of PDA material. When the environmental temperature is higher than the activated temperature of PDAs, its visible light absorption intensity varies continuously as the surrounding temperature rises, and hence the color of the materials presents a series of intermediate states that can be recognized by the naked eye[173] (Figure 11(a)). To prepare PDAs with different activated temperatures, reversibility, and thermostability, plenty of molecular modification methods are proposed[174]. The variation in head groups[175], alkyl side chains[146], and the position of conjugate diacetylene[176] may affect the thermochromic behaviors of PDA materials. Therefore, it is facile to fabricate chemosensors based on PDAs for monitoring the internal overheating of equipment and the environmental temperature in a variety of scenarios. Peng et al.[177] manufactured a robust thermochromic composite material by incorporating artificial nacre onto montmorillonite substrates and introducing the PDA thermochromophore into the composite. The visible absorption peak of the material gradually shifts from 620 to 530 nm with consecutively increasing the temperat-

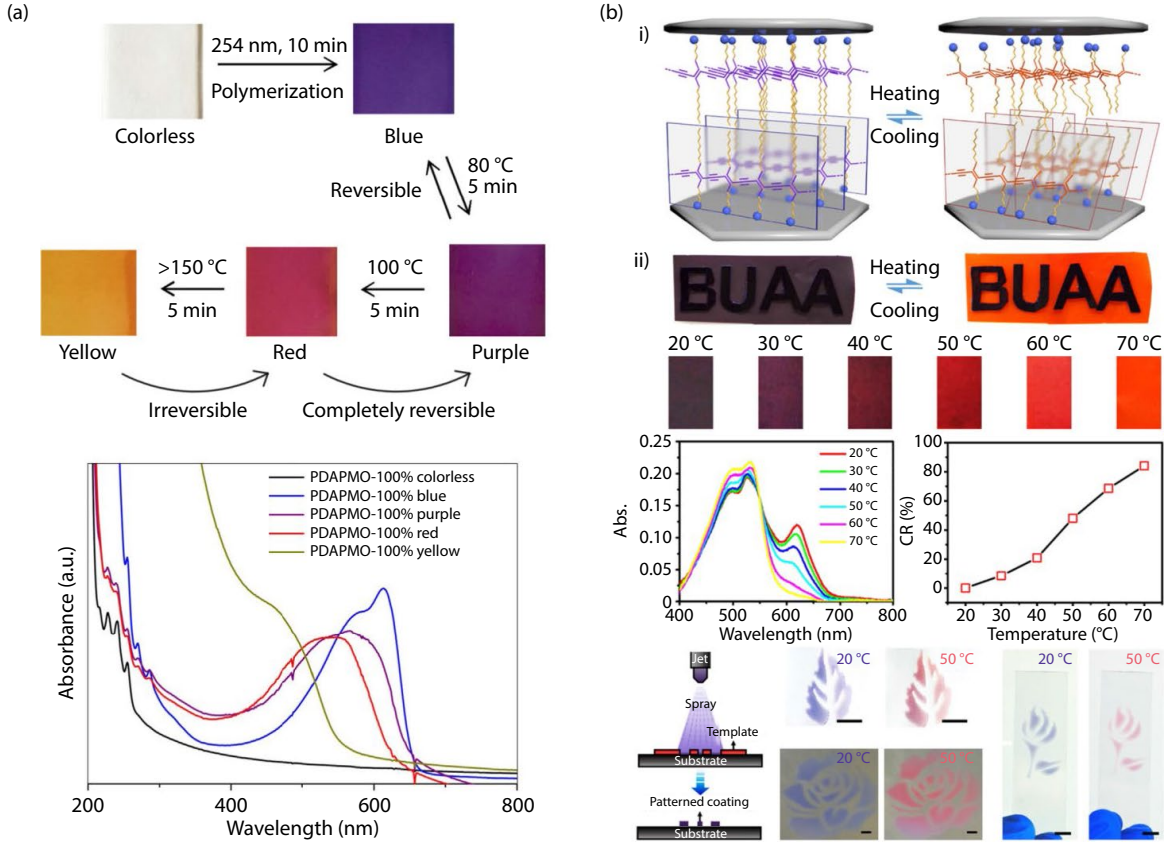

Fig. 11 Thermochromic phenomena of chemosensors based on PDAs. (**a**) Thermochromic behaviours of a type of polydiacetylene-based periodic mesoporous organosilica films (PDAPMO-100%) and their UV–Vis absorption spectra of the colorless, blue, purple, red, and yellow states (reproduced with permission from ref. [173], © 2017 Elsevier). (**b**) Thermochromic artificial nacre based on montmorillonite. (i) Illustration of thermochromism of the artificial nacre. (ii) Reversible thermochromism, UV–Vis spectra, and CR values between 20 and 70 °C. (iii) Illustration of the spray coating via a spray gun, and different artificial nacre patterns inkjet-printed on paper, glass slide, and steel plate. All these artificial nacres show reversible thermochromism between 20 and 50 °C. Reproduced with permission from ref. [177], © 2017 American Chemical Society.

ure from 20 to 70 degrees Celsius, and thus the color undergoes multiple changes from purple to red (Figure 11(b)).

When PDA is exposed to organic solvents, the interaction between the solvent molecules and the pendant groups induces a deformation of the backbone and gives rise to solvatochromism. This behavior is usually nonspecific and related to the polarity of the environment, that is, the degree of distortion of backbone and color variation depends on the polarity of solvents rather than specific organic molecules. Therefore, it is intractable to distinguish different solvents with comparable polarities by observing the color or the spectrum of PDA sensors. Similar to thermochromism, modifying the headgroups can change the solvatochromic behaviors of PDA in an identical solvent. As a result, preparing a group of PDAs with different solvatochromic behaviors is an effective strategy to identify solvents with approximate polarities. Park et al. deposited four diverse PDAs onto the conventional paper by an inkjet printer to form a detect array, which exhibits various color patterns ("fingerprint") in response to 11 organic solvents[178]. Comparing the color response of the PDA array with the fingerprint of each solvent, an unknown solvent could be established.

The intermolecular forces due to mechanical deformation in the polymeric matrix transfer to the backbone of PDA, leading to the reduction of the conjugation length and a mechanochromism. This property is useful to detect certain analytes. For example, saturated aliphatic hydrocarbons (SAHCs) are difficult to directly induce a solvatochromism on account of the nonpolarity of the solvent molecules and the lack of functional groups that can interact with the PDA probes. Park et al. exploited the mechanical stress by the swelling of a PDMS matrix successfully induced a color transition of PDA that was physically incorporated into PDMS films[179] and microbeads[180]. They also discovered that the faster swelling of PDMS due to the hydrocarbons with a shorter alkyl chain activated the PDA molecules to display a color shift from blue to red more rapidly. This stimuli-chromic phenomenon is helpful to contrast different alkyl chain lengths. In addition, Seo et al. reported that the swelling by the interaction between a dry hydrogel matrix and water could induce PDA nanofibers of which the pendant groups were chemically incorporated to the hydrogel ions to present a significant color change[181].

PDA can be photo-triggered as well by grafting photo-responsive compounds to the headgroups of side chains and doping photo-sensitive moieties that can interact with the headgroups into the matrix. The variation in physical and chemical properties of the photo-responsive moieties by light irradiation impact the interaction with PDA backbones, driving a blue-to-red colorimetric transition. Baek et al. reported a reversible photochromism of PDA crystal of which the headgroups were modified by azobenzene[182]. The trans-cis isomerization of azo groups undergoing UV illumination and hydrogen bonds provided by amines led to a color switch and crystal tearing phenomenon.

The poor electrical conductivity hinders electrons from inducing a backbone deformation, therefore the external electric field is difficult to drive an electrochromism of PDA. An effective solution is to prepare a carbon nanotube (CNT)/PDA composite with a higher conductivity by inducing polymerization of diacetylenic precursors on CNT surfaces (Figure 12(a))[53]. When current flows through the CNTs, the hopping of electrons among CNTs changes the interactions of PDA side chains, leading to the PDA backbone being distorted and the conjugation length decreasing. Zhang et al. reported a current-triggered irreversible electrochromism of PDA-PMMA graphene composite materials[183]. They

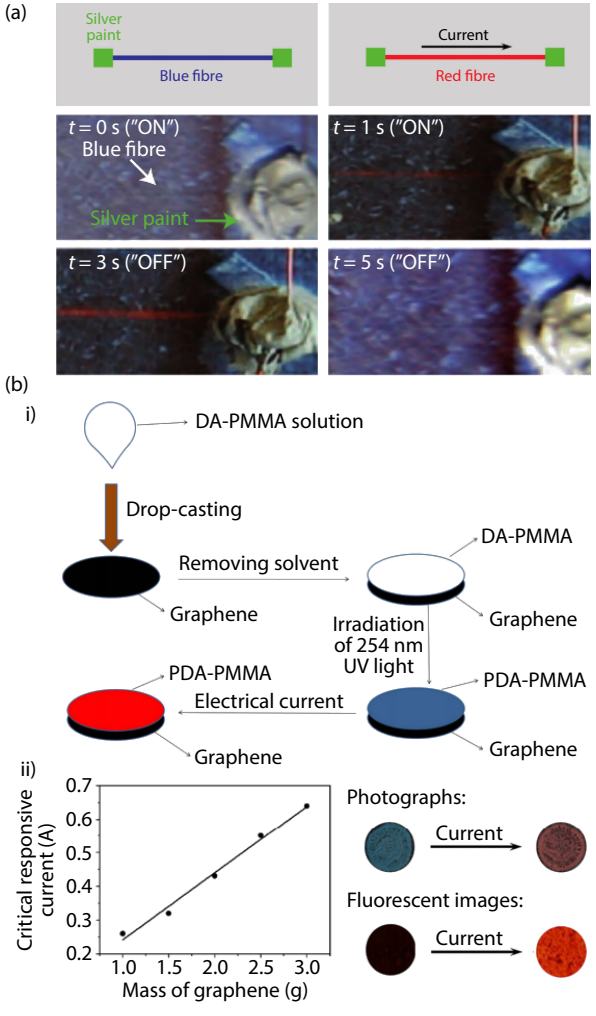

Fig. 12 Current-induced color transition phenomena of chemosensors based on PDAs. (**a**) Chromatic transitions of a composite CNT/PDA fiber in response to an electric current (reproduced with permission from ref. [53], © 2009 Nature Publishing Group). (**b**) Polydiacetylene-polymethylmethacrylate/graphene composites as an electrical current sensing material. (i) Schematic diagram for the preparation of PDA-PMMA/graphene composites followed by the electrochromic process. (ii) Relationship between the critical responsive current and the graphene content. (iii) Photograph and fluorescent image for PDA-PMMA/graphene composites before and after a current stimulus. Reproduced with permission from ref. [183], © 2013 American Chemical Society.

discovered a linear relationship between the graphene mass and the critical responsive current, which is crucial to adjusting the stimuli-chromic behaviors of the composites (Figure 12(b)).

The interaction between the headgroups and analytes can disturb the PDA backbones and result in an affinochromism, which is another extensively explored and widely utilized characteristic of PDAs. Decorating headgroups aiming at specific chemical and biological analytes endows PDAs with high selectivity for detecting the targets. Song et al. realized a rapid visualized detection of the H1N1 influenza virus by employing peptide-functionalized polydiacetylene nanoparticles[184]. The specific binding between peptide groups and the HA1 protein on the virus distorted the PDA backbones. And the deformation was more and more distinct as the virus concentration increased, and thus the nanoparticles exhibited a color transition from blue to purple and ultimately to red.

2.3 Self-reporting materials based on encapsulated systems

In self-reporting materials using encapsulated systems, the encapsulating containers isolate indicator solutions from the polymeric matrix, and thus the detrimental interactions between microencapsulated indicators and media are maximally eliminated. The microcracks in bulk polymers and bruises on their surfaces rupture the encapsulating containers, and the indicator solutions are released into the void of damage or overflow to the impaired surfaces. The disengaged indicators are subsequently triggered by external stimuli, leading to a change in color, fluorescence, or luminescence[144]. This type of material is commonly employed to visualize the mechanical damage in polymers, bruises on surfaces, and metal corrosions for microcrack detection, structure health monitoring, and catastrophic failure prevention of aerospace, automotive, civil engineering, and wind-turbine applications.

According to the type of encapsulating containers, the encapsulated systems are divided into three categories, that is, microcapsules, hollow fibers, and vascular systems. Microcapsules constituted by hollow sphere polymer shells are widely focused, extensively explored, and intensively utilized containers in the aspect of imparting mechanochromic and self-reporting capabilities to materials[105]. The synthesis proceedings of microcapsules mainly include emulsion of the cores and polymerization of the shells[185]. During this process, the hydrophobic core materials are added into the aqueous stirred rapidly to form an o/w emulsion. Then the polymerization is triggered at the interface of the water and the oil phase to form a shell wall. By embedding the indicator-filled microcapsules into the polymeric matrix, a self-reporting material with the ability to detect mechanical damage can be manufactured. Hollow glass fiber is another popular container implemented to store and release indicators, which is usually incorporated into non-reinforced plastics[186]. The fiber not only possesses excellent compatibility with a variety of polymers but also can enhance the mechanical properties of the matrices. Compared with microcapsules, hollow fibers can report and repair damage more efficiently due to larger storage of indicators and healing agents. Microchannel and vascular networks with more complicated 2D or 3D structures can realize multiple autonomous repairs of damage on a larger scale[187]. Similar to circulatory systems, all indicators and healing agents are connected, hence they can migrate freely and replenish efficiently.

White et al. realized autonomous healing of polymers by fabricating microcapsule/polymer composites[188]. The encapsulated healing agent was released from the ruptured microcapsules before the polymerization of the agent was activated by a catalyst embedded into polymers in advance. To visualize the self-healing process, a red dye was encapsulated into the containers simultaneously. Nevertheless, it was difficult to distinguish microcapsules and microcracks by the naked eye, because both of them displayed a red color. To increase the color contrast between damaged and undamaged regions, a strategy of encapsulating switchable indicators was proposed. In this strategy, the inactivated indicator constrained in the containers was supposed to be colorless and present a bright color after it was released into the damaged sites and triggered by external stimuli, such as pH, UV light, catalyst, etc.

Vidinejevs et al. reported a pH-induced self-reporting strategy for visualizing microcracks in both acrylic resin[189] and fiber-reinforced composite[190]. In this strategy, the microencapsulated crystal violet lactone leuco dye isomerized to a blue ring-opened form in an acidic environment provided by silica gel or methyl 4-hydroxybenzoate. Li et al. employed 2′,7′-dichloro-fluorescein (DCF) as a pH-switchable indicator to prepare a type of material with the ability to autonomously report damage[191]. The acidic DCF released to the resin matrix was induced to a basic form in a basic surrounding provided by residual amines, leading to a color shift from light yellow to bright red at the damage site (Figure 13).

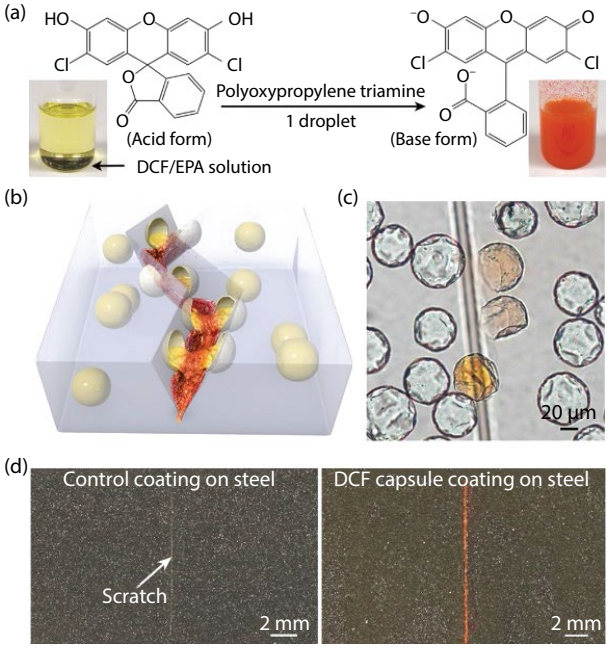

Fig. 13 A pH-induced self-reporting polymeric coating for mechanical damage indication. (**a**) DCF color change indicating mechanism. (**b**) Schematic of autonomous damage indication concept. (**c**) Optical images of microcapsules immersed in curing agent. Color develops when the core materials are released by rupture of the capsule shell wall. (**d**) Optical image of control epoxy coating with no capsules (left) and epoxy coating with 10 wt. % DCF microcapsules (right) on steel substrates with identical scratches. Reproduced with permission from ref. [191], © 2016 WILEY -VCH Verlag GmbH & Co. KGaA, Weinheim.

Credico et al. fabricated a UV-induced self-reporting material by embedding microcapsules consisting of UV-responsive core and UV-absorbing shell into the polymer matrix[192]. The unconstrained indicators released by containers were directly exposed to UV irradiation, while the encapsulated cores were protected by the shells from being triggered. As a result, a photochromism that could be facilely observed by the naked eye occurred in the deteriorated site (Figure 14). Postiglione et al. manufactured a type of self-sensing material based on microcapsules composed of UV-shielding shells and fluorescent liquids[193]. Similar to the photochromic cores mentioned above, only if the core materials were released from the ruptured capsules, the photofluorescent process took place without the protection of shells. Therefore, a UV-induced blue fluorescent emission could be detected from the locations of microcracks.

Odom et al. reported a novel damage sensing strategy by using a catalyst to initiate polymerization and generate colored conjugated polymers[194]. To be precise, the microcapsules containing 1,3,5,7-cyclooctatetraene (COT) monomer and Grubbs–Love (GL) catalyst were dispersed into the polymeric matrix. The nearly colorless COT monomers induced by GL catalyst underwent ring-opening metathesis polymerization to produce the red polyacetylene, which made a distinct color contrast between damaged and healthy polymers. Robb et al. utilized the aggregation-in-

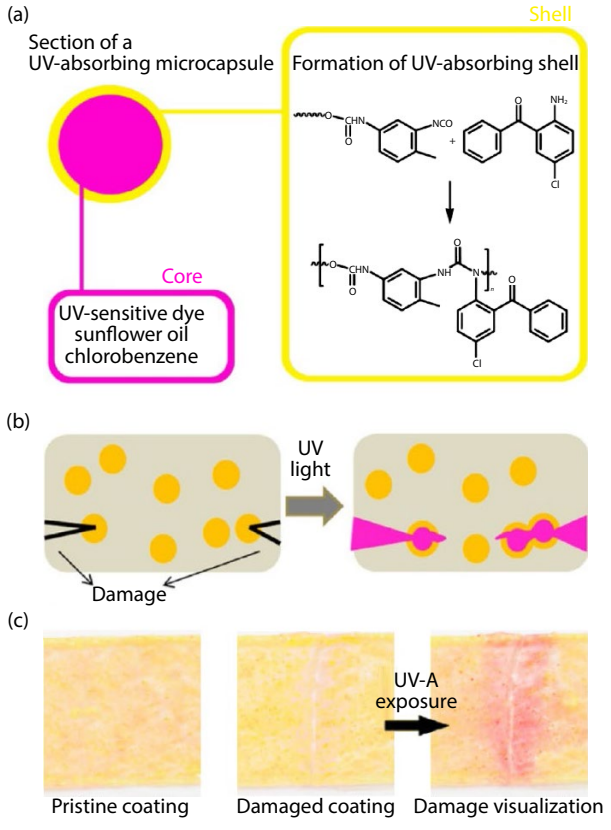

Fig. 14 A UV-induced self-reporting coating based on UV-absorbing microcapsules with photochromic payloads. (**a**) Schematic cross-section of the synthesized micro-capsules with main constituents and shell formation scheme. (**b**) Schematic representation of the visual identification of the mechanical damage by exposure to UV-A light. (**c**) Damage visualization process of microcapsule-containing self-reporting films. Reproduced with permission from ref. [192], © 2013 American Chemical Society.

duced emission (AIE) effect to develop a physically activating self-reporting material for indicating mechanical damage[195]. The microencapsulated AIE luminogens presented no fluorescence when dissolved in an appropriate solvent, but an emission turned on after they precipitated from the solvent due to their intramolecular motions being restricted. Hence, the excurrent core materials exited by UV illumination emitted a blue fluorescence after solvent evaporation. Lavrenova et al. proposed a microencapsulating self-reporting method for visualizing the mechanical deformation and damage based on charge-transfer complexes[196]. The donor and the acceptor were individually encapsulated into microcapsules and uniformly dispersed into PDMS. The incorporation of the two core materials upon deformation or damage led to a color variation from yellow to red in the polymeric matrix.

Chen et al. recently developed a self-reporting material containing dual-compartment microcapsules for mechanical stress and microcrack visualization[197]. Two distinct payloads were encapsulated into different compartments of identical microcapsules in their scheme. Due to the extremely short diffusion distances for the two-component reaction, the color changed more rapidly and significantly at the damaged site compared with the traditional double-microcapsule self-reporting tactics (Figure 15).

2.4 Outlook for SRDs

The ideal self-reporting dielectrics are expected to possess capabilities of expeditiously reporting, significantly responding, and

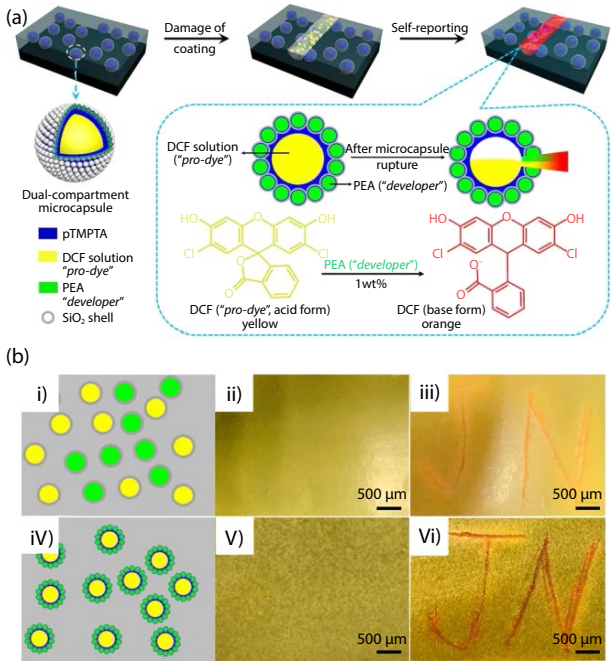

Fig. 15 Robust damage-reporting strategy enabled by dual-compartment microcapsules. (**a**) Schematic diagram of the self-reporting material with dual-compartment microcapsules and its damage visualization mechanism. (**b**) Damage visualization effects of the self-reporting material based on double microcapsules (i) and dual-compartment microcapsules (iv). Reproduced with permission from ref. [197], © 2021 American Chemical Society.

precisely diagnosing. Once the unacceptable insulation degradation or environmental deterioration occurs, SRDs are supposed to immediately display changes in color, fluorescence, or luminescence to report latent risks of catastrophic failure. The variation of optical properties should be easily identified by the naked eye or optical monitoring devices without any ancillary equipment. To eliminate both false-positive and false-negative results, a reasonable response threshold is supposed to be preset, as well as the activated chromophore or fluorophore of SRDs should be switched off after material performances or environmental conditions return to normal levels.

Three stages of SRDs from concepts to applications are depicted as follows. In highly controlled and optimized laboratory conditions, SRDs for various scenarios such as external insulation of insulators, internal insulation of cables, and major insulation of electric machines are expected to be developed. To enter the commercial sector, a lot of efforts are required to maintain the self-reporting functions of SRDs in complicated external environments, and high enough stability and fatigue resistance of the polymeric matrices in the lifecycle. Furthermore, SRDs are expected to be fused with artificial intelligence technology, such as machine perception and computer vision. An advanced system for autonomously monitoring and prewarning the performance of dielectrics in diverse scenarios can be constructed in the future.

3 Self-healing dielectrics

Self-healing mechanisms are quite universal in living organisms, which make it possible to maintain a stable physiological environment and reestablish normal functions of life. From fixing miscreated molecules (such as DNA or proteins) to regenerating cells and tissues, self-healing endows creatures with the ability to resist internal or external damage and a prolonged lifespan. As damage

resistance and long lifetime are also ideal characteristics for non-living materials, much effort has been made in order to introduce self-healing property into synthetic materials. To date, a variety of self-healing approaches have been proposed, including microencapsulation, reversible bonds and interactions, physical interdiffusion, etc[198,199]. However, most of the current research focused on the healing of mechanical damage, in which fracture load and other mechanical properties were used to evaluate the efficiency of healing. With the emerging trend of designing intelligent insulating materials, the self-healing of insulation polymers is attracting more attention. Recent advances in recovering dielectric properties and insulating strength have shown great potential for enhancing the reliability and durability of power insulations and shed light on possible industrial applications in the near future.

In this section, we begin with a comparison between mechanical damage and electrical damage. The special characteristics of electrical damage are highlighted, which should be taken into account when designing self-healing dielectrics (SHDs), particularly when trying to utilize conventional self-healing strategies. Next, we will take a closer look at some recent advances on SHDs. By analyzing their origins and predecessors that heal mechanical damage rather than electrical ones, we will focus on the improvements that make them suitable for insulating materials. We conclude the discussion by summarizing possible paths and the next challenges of designing SHDs.

3.1 Considerations on developing SHDs

Apart from mechanical damage including cracking and fractures, insulating materials may also suffer from electrical damage while working under a high electric field. A typical form of electrical damage is electrical treeing, which seriously affects the reliability and lifetime of insulating apparatus[9]. Unlike direct breakdown that occurs almost simultaneously with overvoltage, the treeing process in solid dielectrics often proceeds under normal operating voltage and lasts for a much longer time.

Electrical trees are often initiated at sites with high electrical stress, especially where moisture, voids, or other contaminants are present[48]. When the local electric field at these sites exceeds the electrical strength of the polymer matrix[200], some electrons are accelerated and collide with polymer chains, resulting in bond scission and free radicals. As the degradation process continues, microcavities appear where partial discharges can take place, leading to a rapid growth of tree channels[9]. Ultimately, the electrical tree will become a fractal system with dendritic hollow channels. During the process of treeing, dielectric properties and insulating performance of polymers are adversely impacted, while the risk of catastrophic electrical breakdown also increases abruptly[48].

When developing self-healing insulating materials, a desirable healing system should be applicable to both mechanical and electrical damage. The scale of electrical trees often lies in micrometers, whereas self-healing of mechanical damage is always tested in the range of millimeters or more. Thus, when adapting current self-healing methods for insulating materials, it should be one of the most important aspects to consider whether the techniques are capable of electrical damage.

Moreover, simply refilling the hollow tree channels is not the end of discussion. While mechanical strength plays an important role in insulating materials, insulation parameters should predominate. The ability for insulating materials to self-heal can only be proved by recovering insulation properties, including breakdown strength, electrical resistivity, etc. Additionally, the incorporated healing agents should not impair the insulating performance of polymer matrix in a significant way.

In addition to the above-mentioned factors, Yang et al. have also proposed other challenges in designing self-healing dielectric polymers[201]. Elimination of chemical degradation products and competence in healing after a long waiting time (time period between damage and applying the conditions required for healing) are ideal features for self-healing insulating polymers. However, only a few studies have considered and tested on these issues, suggesting that further research is still needed in this emerging field.

Besides the considerations on designing proper self-healing methods with high healing efficiency and adaptiveness, SHDs are also desired to be manufactured and recycled easily in order to fulfill whole lifecycle control. However, these issues have not received much attention so far, since there is still some way to go before SHDs can be utilized in practical applications.

To conclude the introduction to electrical damage, it is also worth clarifying the self-healing properties we are discussing here. Decreases in sizes of electrical trees after removing the applied voltages were observed in various polymers, including crosslinked polyethylene, silicone gels and silicone rubbers[47,202,203], which were also referred to as "self-healing" in some literature. However, these phenomena were attributed to the elasticity and mobility of polymer chains, rather than establishing firm chemical interactions. In the absence of complete removal of tree channels, re-formation of chemical bonds, and full recovery of insulation properties, these phenomena cannot be used in developing self-healing insulating materials, and are therefore excluded from our discussion.

3.2 Melting interdiffusion by magnetic heating of nanoparticles

When subjected to an oscillating magnetic field (OMF), magnetic nanoparticles will undergo an energy dissipation process and generate heat owing to Brownian and Néel relaxations[204,205]. By introducing magnetic nanoparticles into polymer matrix, self-healing of mechanical damage in various thermoplastic polymers has been illustrated[206–209], a schematic of which is shown in Figure 16(a). With an elevated temperature under OMF treatment, the polymer would melt and flow to close the cracks, enabling chain diffusion and randomization which leads to restoration of mechanical properties[206,210]. A fraction of at least 3.5 wt. %[208] or 1 vol. %[209] of magnetic nanoparticles is reported to obtain satisfactory self-healing performance, which can be detrimental to the insulation properties of polymers.

A recent breakthrough was made by Yang et al. in integrating melting interdiffusion self-healing ability into thermoplastic dielectrics while still maintaining their insulation properties[54,211]. One of the key aspects of this method was endowing magnetic nanoparticles with the potential to migrate towards microcracks, which is analogous to the hemostasis mechanism of vascular injury in our bodies. Upon a blood vessel injury, signal transduction process is activated with platelets aggregating at the site of injury. With the aid of fibrin, the platelets are packed together, forming blood clot to prevent further bleeding (Figure 16(b)). Fast-acting hemostasis prevents the situation of injury from worsening and allows for a mild and stable environment for cell regeneration and self-healing. Different from the bioinspiration where signal molecules are transmitted to initiate aggregation, entropic depletion is the key factor in the defect-targeted self-healing strategy.

In polymer nanocomposite systems, the conformational entropy of polymer chains in the vicinity of nanoparticles is reduced due to spatial confinements[212]. Thus, it will be entropy-favourable

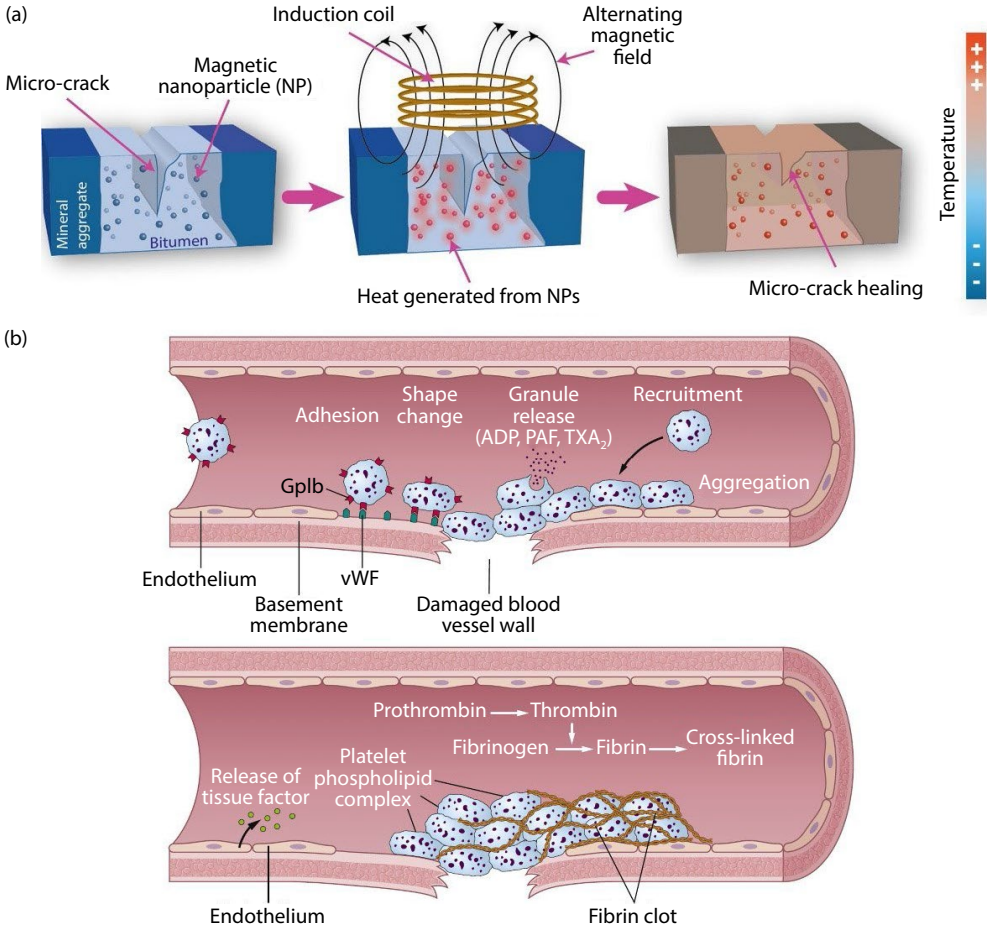

Fig. 16 Inspirations for designing self-healing dielectrics by melting interdiffusion. (**a**) A schematic of healing mechanical damage by incorporating magnetic nanoparticles in bitumen matrix. A treatment of oscillating magnetic field is required (reprinted with permission from ref. [209], © 2016 Elsevier). (**b**) The self-healing process of a vascular injury. Platelets aggregate at the injury site and form clot to stop bleeding. The aggregation behaviour of platelets serves as a bioinspiration for defect-targeted self-healing strategy (reprinted with permission from ref. [215], © 2020 Elsevier).

to "squeeze out" the particles, resulting in aggregation of nanoparticles towards microcracks[213,214]. Two factors need to be emphasized for this entropic depletion phenomenon. The first one is the miscibility between nanoparticles and polymer matrix. Both enthalpic and entropic interactions between polymer chains and nanoparticles are accountable for the particles' behaviour. When the miscibility is poor, enthalpic interactions will dominate and suppress the forming of a uniform nanocomposite[213]. Only good compatibility will make it possible for entropy interactions to exert influence. The size of nanoparticles also plays a significant role, since the entropy penalty must be strong enough for the migration of particles to proceed. The segregation of nanoparticles to cracks could only be observed for particles of at least a size comparable to the gyration radius of polymer chains[214].

The defect-targeted self-healing method for thermoplastic polymers developed by Yang et al., as shown in Figure 17(a), is competent for both electrical and mechanical damage[54]. Superparamagnetic nano-particles, with the ability to migrate to defect sites, were incorporated in commercial polypropylene (PP). After electrical treeing, the specimen was treated with OMF for self-healing. The nanoparticles were observed to concentrate around the tree channels, generating heat and resulting in melting interdiffusion (Figure 17(b)). After healing of damage, the nanoparticles could redisperse in the matrix, enabling the next healing phase. Electrical properties including leakage current, partial discharge magnitude (Figure 17(c)) and tree inception voltage effectively recovered to the same level before electrical aging. Further investigations confirmed the validity of this defect-targeted method in healing mechanical damage and in different thermoplastic polymers, such as polymethyl methacrylate (PMMA) and perfluorosulfonic acid (PFSA)[211].

By integrating the advantages of magnetic interdiffusion and nanoparticle migration, the content of nanoparticles is as low as 0.09 vol. % could satisfy the self-healing need without influencing the polymer's electrical insulation and dielectric properties[54]. This merit came from the trend of particle migration since the nanoparticles and heating power could concentrate at the damaged site. The nanoparticles served only as heaters, so they would not be consumed or exhausted, endowing the nanocomposites with a highly repeatable healing ability with a long waiting time. It was still possible to achieve a healing efficiency of over 90% even after 100 cracking-healing cycles (Figure 17(d)) or 100 days of waiting time[211].

It is worth mentioning that surface functionalization was quite essential in this emerging approach[54]. The type of surface modifiers was chosen to enhance the compatibility between nanoparticles and polymers, which is a prerequisite for entropic depletion. The thickness of functioning layers was optimized to match the gyration radius of polymer matrix while maintaining a relatively high mobility. The surface functioning layers also provided a

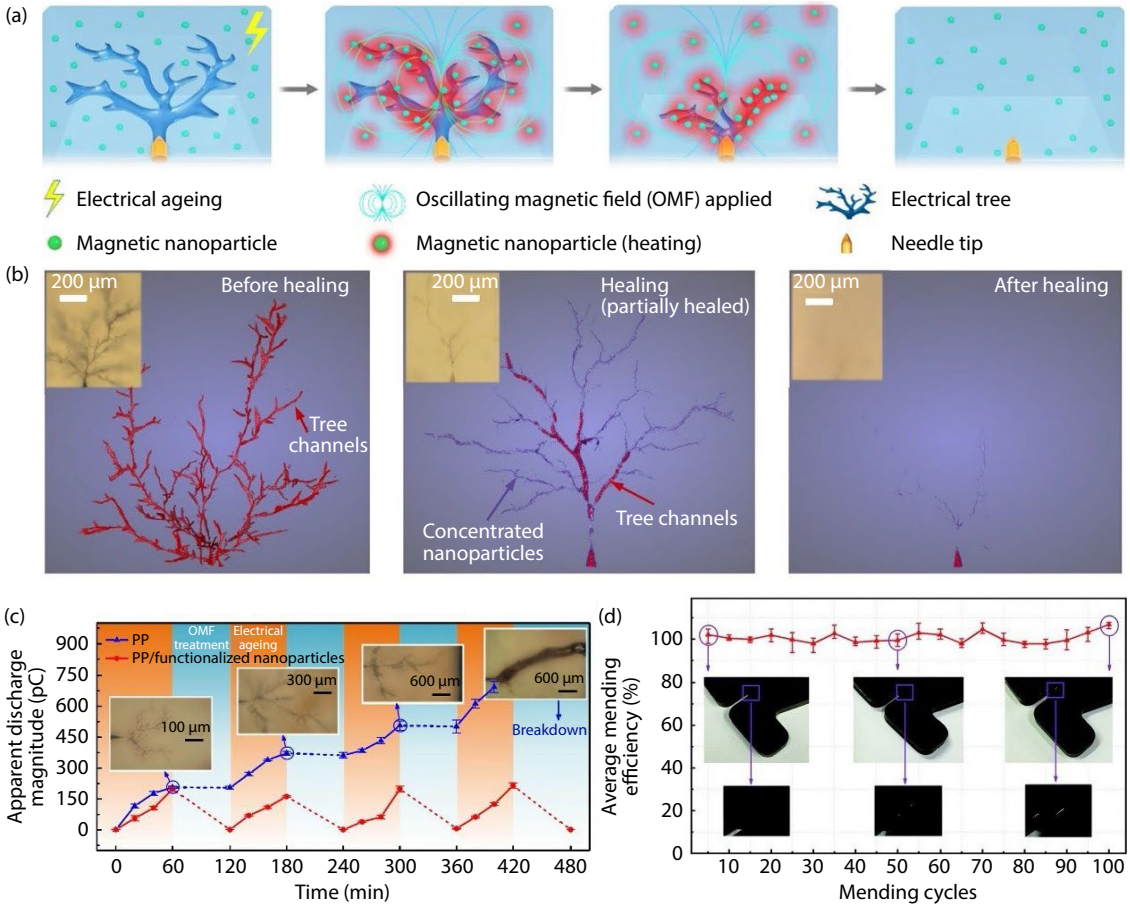

Fig. 17 Defect-targeted self-healing insulating materials. (**a**) A schematic of healing electrical trees by incorporating superparamagnetic nanoparticles. When treated by an oscillating magnetic field, the nanoparticles will migrate toward tree channels and generate heat, leading to melting interdiffusion at the damaged site (reprinted with permission from ref. [54], © 2018 Springer Nature). (**b**) The reconstruction of electrical trees in polypropylene (PP) during self-healing process by computed micro-X-ray tomography (reproduced with permission from ref. [54], © 2018 Springer Nature). (**c**) Apparent partial discharge magnitude of PP specimens with and without magnetic nanoparticles during multiple aging-healing cycles (reprinted with permission from ref. [54], © 2018 Springer Nature). (**d**) Healing efficiency for mechanical damage in 100 cracking-healing cycles (reprinted with permission from ref. [211], © 2020 The Royal Society of Chemistry).

steric repulsion to prevent permanent aggregation.

The main restrictions for this defect-targeted self-healing method lie in the polymer matrix and the healing stimuli. Melting interdiffusion requires a thermoplastic matrix so that the molten polymer can flow into microcracks. The healing temperature must exceed the polymer's glass transition temperature to ensure nanoparticles' mobility. OMF with high intensity and frequency may also pose a barrier against practical application of this method. Nevertheless, this emerging method is still promising in power transmission systems or power electronics where OMF exists or can be easily applied[54]. By finely tuning the composition and size distribution of nanoparticles[205,216], an increased heating power can also lead to broader applications for this self-healing mechanism.

3.3 Microcapsule-based SHDs

(a) General considerations

Starting from designing autonomic healing polymer composites by using dicyclopenta-diene (DCPD) and Grubbs' catalyst[188], extrinsic self-healing methods based on microcapsules have been widely and intensively studied. The encapsulated healing agents are released and begin to polymerize when capsules are ruptured by damage. Nearly all kinds of polymerization chemistries have shown great potential in healing mechanical damage[217,218]. However, when it comes to self-healing of electrical damage, current research is still limited. Some concerns about developing microcapsule-based self-healing insulating polymers are as follows.

Microencapsulation self-healing methods can be further divided into different categories according to the form of healing agents (monomers) and catalysts or initiators[217]. Although capsule-catalyst systems and multi-capsule systems perform well in healing mechanical damage, they are not so favourable when dealing with electrical trees in much smaller sizes, since the possibility of electrical trees contacting catalysts or all types of microcapsules will be much lower than in the case of mechanical damage[201]. Additionally, this issue cannot be resolved by raising the content of microcapsules or catalysts. When the concentration of microcapsules exceeds a certain limit (usually about 5 wt. %), a sharp deterioration would be observed in both mechanical and electrical properties, including tensile strength, dielectric loss, and electrical breakdown strength[219–221]. On the other hand, the addition of catalysts and other small molecules may distort local electrical field and serve as defects and contaminants, resulting in easier initiation of electrical trees and worse insulating properties[222–224].

Despite that the content of microcapsules needs to be controlled strictly to preserve satisfactory performance of the polymer matrix, the micro-encapsulation approach has its unique advantage of attracting the route of electrical trees, making the rupture of

capsules more likely. The incorporated microcapsules may lead to charge accumulation and electric field distortion, thus influencing the electrical tree routes in their vicinity. Lesaint et al. tested the healing system of DCPD and Grubbs' catalyst in epoxy resin with electrical treeing[225], finding the trend of tree channels to be attracted by microcapsules. Wang et al. investigated the same system in polyethylene[219] and verified the attraction effect again. However, no apparent evidence of complete recovery of hollow tree channels or electrical properties were reported in both studies, which might be attributed to the disadvantage of capsule-catalyst system mentioned above. Computer simulations have also revealed that capsules with a higher dielectric constant and higher electrical conductivity than the matrix would have a remote attraction effect on tree trajectories, whereas capsules with a lower breakdown strength could attract electrical trees in a shorter range[55]. However, it needs to be noted that the attraction of tree trajectory towards microcapsules should not be overused, otherwise the polymer matrix would possibly suffer from performance degradation[55]. The balance between self-healing validity and insulation properties of polymer composites should be considered carefully.

Since capsule-catalyst systems and multi-capsule systems have their inherent shortcomings, the main microcapsule-based self-healing methods that are currently used for electrical damage include polymerization initiated by environmental stimuli and latent functionality strategies. Instead of catalysts, some polymerization chemistries require external stimuli to proceed with or without corresponding initiators. These reactions can be utilized for self-healing to eliminate the detrimental effect of incorporated catalysts. The latter approach uses residual reactive functionality in the polymer matrix as polymerizer[217]. As we will see later, those residual functional groups can actually serve as hardeners for the polymer matrix, guaranteeing satisfying insulation properties of the self-healing material.

(b) Polymerization triggered by environmental stimuli

Various external stimuli, such as moisture, oxygen, and sunlight, have been utilized to trigger polymerization of monomers to design self-healing or other intelligent polymers. The reactivity of diisocyanates with water has been used to form anticorrosion self-healing coatings. By introducing microcapsules containing isophorone diisocyanate into epoxy resin, polymerization was observed in the presence of water and without any catalysts, showing the potential of autonomous self-healing in aqueous or high-humidity environment[226]. The oxidative polymerization of linseed oil has also shown promise in developing self-healing coatings, since linseed oil released from ruptured microcapsules could polymerize when exposed to atmospheric oxygen, preventing further corrosion by external moisture and oxygen[227]. Different systems of monomers and photoinitiators that can initiate the polymerization process under sunlight or ultra-violet (UV) radiation have also been tested for designing self-healing polymer composites or protective coatings[228–230]. Note that in order to maintain long-term effectiveness of photoinitiators and self-healing mechanism, additional measures to absorb radiations before the rupture of microcapsules should be taken. For example, by incorporating TiO_2 nanoparticles, the microcapsule shells possess an excellent photo-absorption function with wide band and high absorbance[229].

When considering a proper stimulus for electrical damage healing, researchers paid much attention to the phenomena and byproducts of electrical aging. Light emission and free radical production are common effects that associated with electrical treeing. Free radicals are generated due to hot electrons' collision into polymer molecules, whereas light emission has several different origins. Various kinds of light can be produced when excited molecules return to ground states and when recombination of opposite charge carriers happens[9]. Partial discharges can also generate light emissions that peak in the UV range[231].

Gao et al. proposed a self-healing approach for electrical defects based on UV light originated from electrical treeing (Figure 18(a))[55]. Epoxy monomer (bisphenol A epoxy acrylate) and reactive monomer (trimethylolhexane triacylate), along with photoinitiator (1-hydroxycyclohexyl phenyl ketone) and SiO_2 nanoparticles, were encapsulated via one-step Pickering emulsion polymerization. Different fractions of microcapsules were then incorporated in epoxy resin to form self-healing insulating composites. The SiO_2 nanoparticles were introduced to adjust the dielectric and insulating properties of microcapsules, thus lessening the negative effect on the properties of epoxy matrix. With a volume fraction of less than 5%, the microcapsules induced an acceptable decline in breakdown strength and electrical resistivity of the self-healing composite. Additionally, TiO_2 nanoparticles were incorporated in the capsule shells to shield UV light, avoiding healing agents from polymerizing before the rupture of microcapsules.

In the electrical treeing experiments, the tree trajectories were observed to be attracted by the nearby microcapsules, which matched the results by computer simulations mentioned above. This characteristic ensured a satisfactory healing efficiency despite a rather low doping fraction. After electrical trees punctured the microcapsules, the healing agents would flow into hollow tree channels, and radical polymerization would be initiated by photoinitiator and UV light from the electrical aging process. The whole process of self-healing needed no external intervention, and could achieve more than 95% volume ratio of healed tree terms of electrical resistance and breakdown voltage were channels ultimately (Figure 18(b))[55]. The insulating properties in recovered upon self-healing, which is the first example of high-efficiency restoration of electrical performance by using microcapsule-based self-healing approaches. Note that the microcapsule-based self-healing of dielectric polymers reported by Lesaint et al.[225] and Wang et al.[219] did not involve any evidence of recovering electrical properties from treeing degradation.

Traditionally, microcapsule-based self-healing methods can only heal once for damage in each location, since the healing agents can only be exposed and reacted once[218]. This issue is partially resolved from a novel aspect in the UV-triggered self-healing method. By adjusting the healing agents, the local insulation properties in the healed sites were even better than the undamaged regions. As a result, new electrical trees would tend to develop in new paths rather than growing along the original trajectories (Figure 18(c))[55]. Hence, the risk of using up healing agents and loss of self-healing ability at one site could be efficiently lowered.

A more recent attempt of developing self-healing insulating materials was made by Sima et al. (Figure 18(d))[232], using the same stimulus of UV light originated from electrical aging, but with completely different healing reactions. Monomers (3,4-epoxycyclohexyl-methyl 3,4-epoxycyclohexanecarboxylate) and photo-initiators (triarylsulfonium hexafluorophosphate salt) were encapsulated and would undergo a cationic polymerization process in the presence of UV light. In addition to TiO_2 nanoparticles, Fe_3O_4 nanoparticles with SiO_2 coatings were also incorporated into the capsule shells, endowing the microcapsules with targeted mobility under a magnetic field. During the hardening process of the epoxy matrix, the microcapsules could be attracted towards

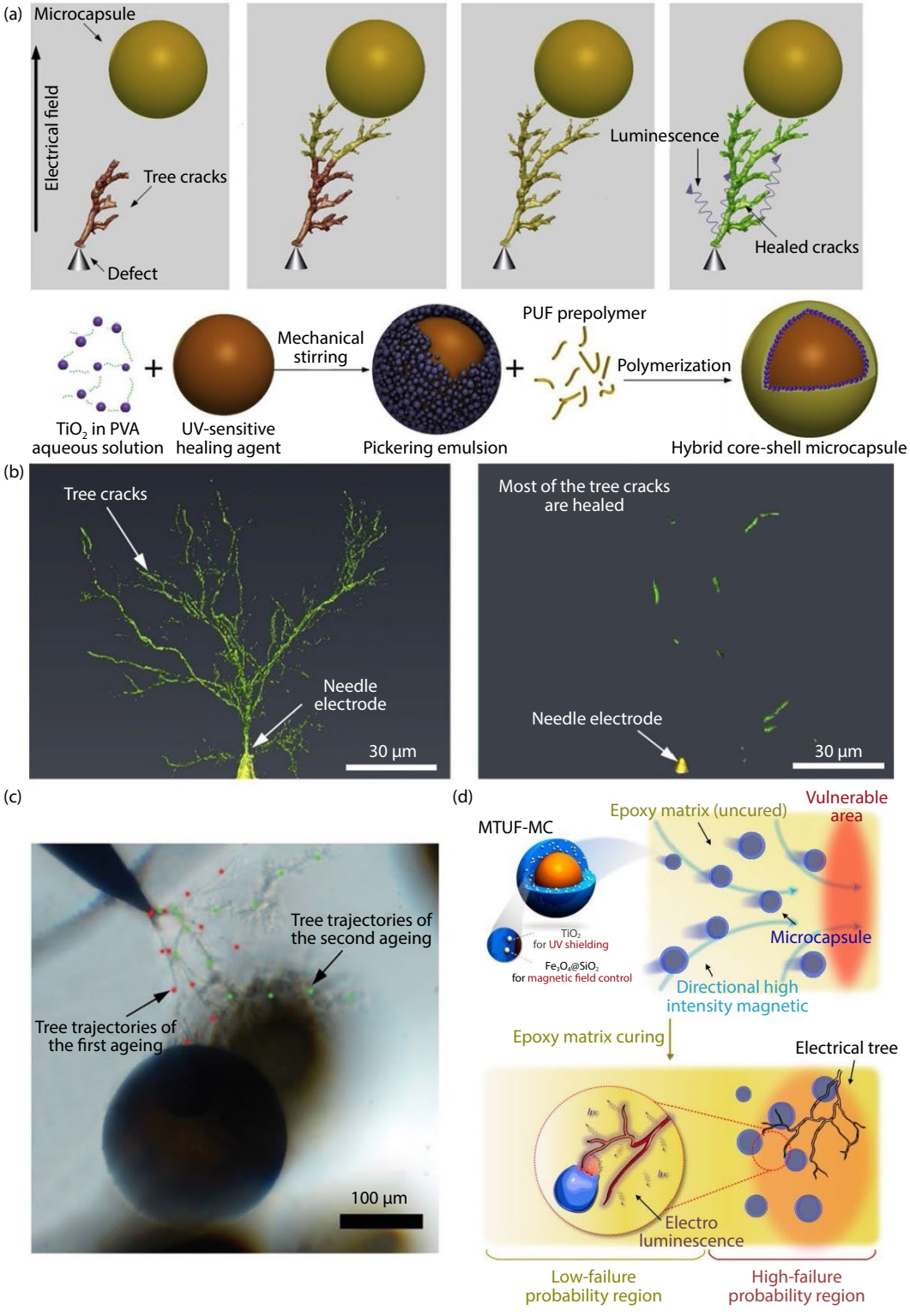

Fig. 18 Microcapsule-based self-healing insulating materials triggered by environmental stimuli. (**a**) The self-healing mechanism using polymerization is triggered by UV light during the electrical treeing process and the preparation of microcapsules. TiO_2 nanoparticles in capsule shells serve as light-absorbing materials (reprinted with permission from ref. [55], © 2019 Elsevier). (**b**) The reconstruction of electrical trees and healed trees in epoxy by computed tomography (reprinted with permission from ref. [55], © 2019 Elsevier). (**c**) Electrical trees developed in new paths in re-treeing process rather than along the trajectories of the first aging phase (reproduced with permission from ref. [55], © 2019 Elsevier). (**d**) Schematic of UV-triggered self-healing method with magnetic targeting. The microcapsules can be guided towards regions with higher electrical stress and failure possibility during manufacturing (reprinted with permission from ref. [232], © 2021 American Chemical Society).

more vulnerable regions by applying a directional magnetic field. Thus, a controllable distribution of microcapsules could be achieved with higher concentration and better self-healing ability in regions with higher electrical stress or stricter working conditions.

The UV-triggered polymerization approaches for healing elec-

trical damage utilize the UV light emitted by electrical aging, which makes the healing process autonomous and intervention-free. However, when dealing with mechanical failure, natural UV light or manual UV radiation treatment will be necessary[232], making these methods less convenient. Furthermore, when electrical aging becomes more severe, carbide residue generated by severe partial discharges will hinder the full recovery of insulating properties[55], showing the importance of eliminating degradation products in healing electrical damage.

The two self-healing methods introduced above both use UV light as stimulus for polymerization, which opens up the prospect of further investigation. For instance, radicals are also generated during electrical treeing, showing a possible path for utilizing free radical polymerization to develop new self-healing insulating materials. Generally, two types of microcapsules are required in self-healing materials based on free radical polymerization, one containing monomers and the other containing radical initiators[233,234]. As for electrical damage healing, radical initiators may be negligible, potentially reducing complexity and enhancing adaptability of this self-healing method.

(c) Polymerization by latent functionality

In the latent functionality route, the polymerizer comes from residual reactive functionality in the polymer matrix[217], such as residual or additionally introduced hardeners for epoxy resin. Based on the latent hardener approach, imidazoles and Lewis acids have been utilized in self-healing epoxy resins that mainly focus on mechanical damage. The cationic ring-opening polymerization between epoxy and Lewis acid BF_3 was exploited to design self-healing fiber-epoxy polymer composites[235]. Microcapsules containing epoxy and latent hardener $CuBr_2(2\text{-MeIm})_4$ (the complex of $CuBr_2$ and 2-methylimidazole) were incorporated into epoxy and fiber-epoxy composites to develop new self-healing materials[236,237]. Since imidazoles are broadly used in industry with good commercial availability and chemical stability, imidazole based self-healing schemes show a high potential for self-healing materials[238].

In the self-healing systems using $CuBr_2(2\text{-MeIm})_4$ by Yin et al., the well-dispersed complex would decompose and release imidazole molecules at high temperatures, enabling the curing reaction between imidazole and epoxy monomers coming out from microcapsules[236]. By using imidazole complex, the reactivity of imidazole could be kept well. However, the remnant of $CuBr_2$ might do harm to the insulating properties after the healing process, which is not desirable in applications of insulating materials. Hart et al. developed another self-healing system by incorporating 2-ethyl-4-methylimidazole (EMI) directly into the epoxy matrix as a latent hardener[238]. To protect the reactivity of EMI for later self-healing, amine curing agent was also added to the epoxy monomers. The initial curing process was conducted under 30 °C, at which temperature the monomers would tend to polymerize with amine agents rather than EMI. During this curing process under low temperature, EMI would only go through the first step of polymerizing, producing EMI-epoxy adduct. After the occurrence of mechanical damage, the composite was heated to about 100 °C, substantially increasing the reactivity of EMI and allowing the remaining steps of EMI-epoxy crosslinking to proceed.

Based on the same reaction principles of EMI and epoxy resin, Xie et al. designed a self-healing method for electrical damage (Figure 19(a))[239]. Epoxy monomer (diglycidyl ether of bisphenol A, DGEBA), primary curing agent (phenol-aldehyde amine, PAA) and latent hardener (EMI) were mixed with microcapsules containing healing agent (another epoxy monomer, diglycidyl ether of bisphenol F, DGEBF) and underwent the first hardening process at a relatively low temperature. Amine curing agent played a major role at this phase while EMI could still maintain its reactivity until self-healing stage at an elevated temperature. A content of less than 3 wt. % of EMI would be sufficient for healing while retaining excellent mechanical and insulating properties of the epoxy matrix (Figures 19(b) and 19(c)).

Similar to the UV-induced self-healing approach, in the latent functionality strategy, it was also observed that microcapsules could attract the tree trajectories and new trees would tend to develop in new regions rather than the healed ones[239]. Additionally, long-term effectiveness was tested by accelerated thermal aging experiments. Although severe oxidation could be deduced from visual colour changes and FTIR results, the EMI-modified epoxy could still trigger self-healing reactions[239], showing decent long-term validity.

Since the working temperature of epoxy-based insulating materials is generally higher than ambient temperature, the EMI-epoxy curing process can be autonomous under appropriate working conditions. In a broader sense, by utilizing different derivatives of imadazoles, maximum reactivity could be obtained at different temperatures. Thus, it will be possible and of great potential to design various self-healing systems that maximize the reactivity of latent functionality at the estimated working temperature for insulations.

(d) Summary

Among all self-healing mechanisms for electrical damage, the advantages of microencapsulation approaches lie in the automatic healing process that can proceed under normal working conditions and without manual intervention. Although it is an intrinsic shortcoming that the healing capacity for one specific location is very limited, better insulating performance at the healed region can possibly reduce the risk of treeing at the same site.

Except for microcapsule-based self-healing, the extrinsic method of vascular networks has also been studied extensively in mechanical damage healing. Compared to microcapsules, vascular networks seem to be a lot more similar to real blood vessels in organisms, with multiple healing cycles at one spot and the ability to refill healing agents externally[217]. However, a vascular self-healing network is more expensive to design and maintain, and causes additional challenges in the manufacture of insulating materials, thus requiring more research before practical applications.

3.4 Reversible crosslinking network

Besides the extrinsic methods, there are also a large set of self-healing methods that use reversible covalent bonds or supramolecular interactions, which can be broken and rebuilt in multiple healing cycles[240,241]. How to make the chemical interactions competent to bond fractured surfaces together will be the first challenge when exploiting intrinsic methods for healing electrical damage.

Generally speaking, there are five stages in a crack healing process: surface rearrangement, surface approach, wetting, diffusion, and randomization[210,242]. The stage of surface approach is what we want to emphasize here. Surface approach is trivial in most self-healing work for mechanical damage, in which the fractured surfaces are often manually held together, and pressure is also applied to ensure intimate contact in some cases. However, in the context of electrical trees, it won't be an easy problem for the separated surfaces to approach and contact each other. In the above-

mentioned electrical tree healing methods, the gap between surfaces is filled with either molten polymer or liquid healing agents.

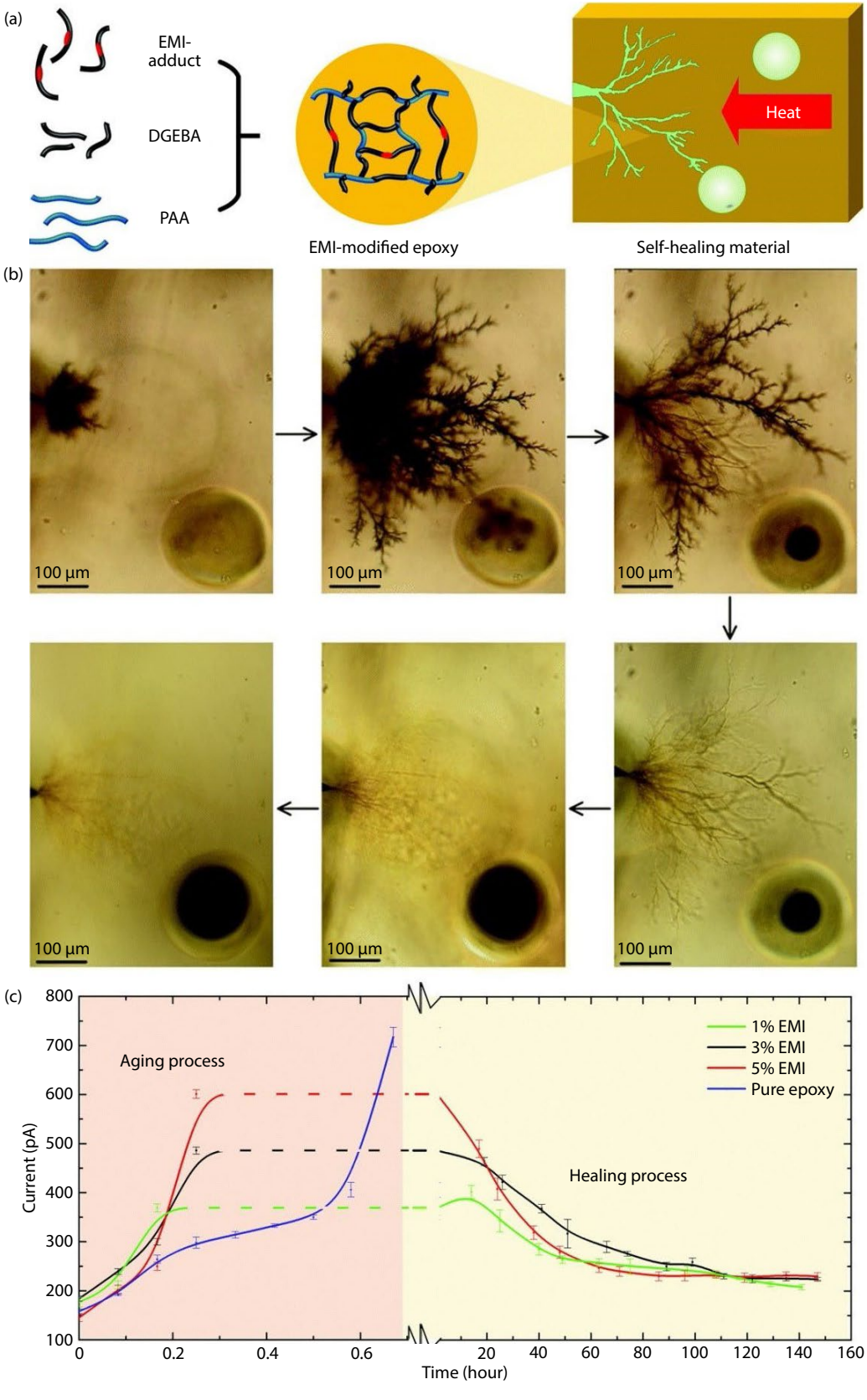

Fig. 19 Microcapsule-based self-healing insulating materials triggered by latent functionality. (**a**) Schematic of fabricating self-healing epoxy by latent functionality. Epoxy monomer DGEBA, primary curing agent PAA and latent hardener EMI were mixed to produce EMI-modified epoxy. Self-healing was obtained by cross-linking of EMI and epoxy monomers from microcapsules. (**b**) Optical microscope images of aging and healing process of self-healing epoxy samples. (**c**) Leakage current of epoxy specimens with different concentrations of EMI during electrical aging and healing. Reprinted with permission from ref. [239], © 2020 The Royal Society of Chemistry.

But in intrinsic systems where interactions can only happen between neighbouring molecules, chain mobility has to take the responsibility to achieve surface approach.

One main challenge faced by intrinsic self-healing lies in the conflict between mechanical stiffness and chain dynamics. Excellent chain flexibility and mobility are required for the effectiveness of self-healing, but they will often result in a lack of mechanical stability[218,243]. Therefore, it will be favourable to design self-healing materials with two states: a working state with sufficient mechanical properties; and a healing state with increased chain mobility. The inspiration of this idea can be traced back to the healing mechanism of hard structures in living organisms such as bones (Figure 20(a)). Bones are hard, dense connective tissues that support structure of the body. The rigidity of bone also makes it difficult to directly repair the tissue. Instead, a soft-to-hard transition strategy is applied[244]. After a bone fracture, a spongy bone is first formed at the damaged site, where the dead bone is resorbed and new cells are generated. Via endochondral ossification, cartilage is gradually replaced by trabecular bone, which can be loosely regarded as a hardening process. Eventually, compact bone will replace the spongy bone and complete the healing.

Based on the two-state tactic, a series of self-healing systems by Diels–Alder (DA) reactions have been realized, where retro-DA reactions depolymerize the crosslinked polymer under elevated temperature whereas DA reactions rebuild the covalent bonds to repair the cracks at a lower temperature[241,245–248]. However, these self-healing polymers share the same drawback of being totally uncrosslinked at the healing state, which may lead to shape changes and performance degradation, especially in applications like insulating materials.

To avoid a completely uncrosslinked healing state, Xie et al. proposed a partially reversible crosslinking epoxy network (Figure 20(b))[56]. The first step was synthesizing the dynamic crosslinker by DA reaction of 3-furoic acid and maleic anhydride. Self-healing epoxy network was fabricated by using the dynamic crosslinker to cure commercial epoxy monomers. Each crosslinker molecule could link up three epoxy monomers, leading to a fully crosslinked network. After internal damage occurred, by heating up to 130 °C, the crosslinker would undergo retro-DA reaction and decompose into furoic acid and maleic anhydride, with only one and two crosslinking points with epoxy chains respectively, forming a partially crosslinked polymer. By reducing the degree of crosslinking, higher chain mobility and more free volume would provide good conditions for self-healing. Moreover, the overall structure and properties of epoxy matrix could be well preserved as the matrix was still crosslinked rather than thermoplastic. Fully crosslinked epoxy could be obtained after the healing stage by lowering the temperature and letting DA reaction take place again. This conversion between fully and partially crosslinking state could be simply controlled by temperature, showing a convenient self-healing method with excellent reversibility.

The partially reversible crosslinking network increased chain mobility during the healing process by partially depolymerization, making it possible for epoxy chains to diffuse into hollow channels and cracks. This method also showed unique advantages in healing electrical damage by eliminating the byproducts of treeing, including gaseous products of chemical degradation and free radicals from chain scission. During the healing stage, augmented free volume inside the polymer would promote the diffusion of gaseous byproducts and hinder their accumulation, while the conjugated double bonds from the dynamic crosslinker could react with free radicals to eliminate them. Self-healing tests showed highly recoverable mechanical strength and insulating properties after more than 10 healing cycles and a decent performance in healing electrical trees (Figure 20(c))[56].

The self-healing epoxy network with partially reversible crosslinking sites shows great potential in practical applications, since modifications may be needed only for curing agents while commercial epoxy monomers can still be used as received. Nevertheless, as chain mobility being the key factor of healing process, the healing efficiency may be less than satisfactory when dealing with large scale defects. Although applying more cycles of heating treatment can improve healing performance[56], it may also detract from the convenience of this self-healing approach.

3.5 Summary for SHDs

In light of the increasing requirements for insulation reliability in power systems, several approaches have been proposed to design self-healing insulating materials. Stringent insulation requirements and special damage forms like electrical trees are the main distinctions that extinguish this field from traditional self-healing materials. Despite that the self-healing methods discussed above are all competent in repairing electrical trees, they are still limited by inconvenient conditions for healing, complicated manufacturing process or inconsistent healing efficiency for different damage scales. In addition, the carbide residues generated by severe discharges are not properly dealt with in these approaches, which may be a hidden trouble for self-healing insulation. Furthermore, while all these self-healing methods are currently tested under laboratory conditions, their self-healing performance and long-term effectiveness are still to be evaluated in practical applications. To summarize, these limitations illustrate that there is still much to be done for insulating materials with intelligent self-healing functions to become a reality.

4 Outlook

Traditional dielectrics encounter a variety of challenges in internal electric field grading, insulation deterioration detection, and electrical damage repairing. In nature, animals and plants have evolved various capabilities of adapting to the environment, detecting injuries, and healing wounds by natural selection for surviving in harsh surroundings. Similarly, developing smart dielectric materials for the next-generation electrical insulation, such as self-adaptive, self-reporting, and self-healing dielectrics, with bio-inspired and autonomous functions is an innovative approach to surmounting the above barriers. At present, bionic smart materials have been applied in a variety of electrical equipment, such as bushing, cable terminals, and insulators. Nonetheless, there are also plenty of obstacles to designing, fabricating, and utilizing smart materials either in the laboratory or in the commercial sector. A lot of effort should be put to turn the concepts into reality.

Three evolutionary stages of smart dielectrics are envisaged in the following. In the early stage, the performance of the smart dielectrics is supposed to be improved in highly controlled and optimized laboratory conditions. Self-adaptive dielectrics with a larger nonlinear coefficient, a switching field that can be flexibly tuned in a wider range, and more stable characteristics against various surroundings such as filler concentration and temperature, are required to be developed. Finding novel field grading principles and manufacturing functional fillers with improved performance are both reasonable alternatives for achieving this goal. Self-reporting dielectrics with the capabilities of expedi-

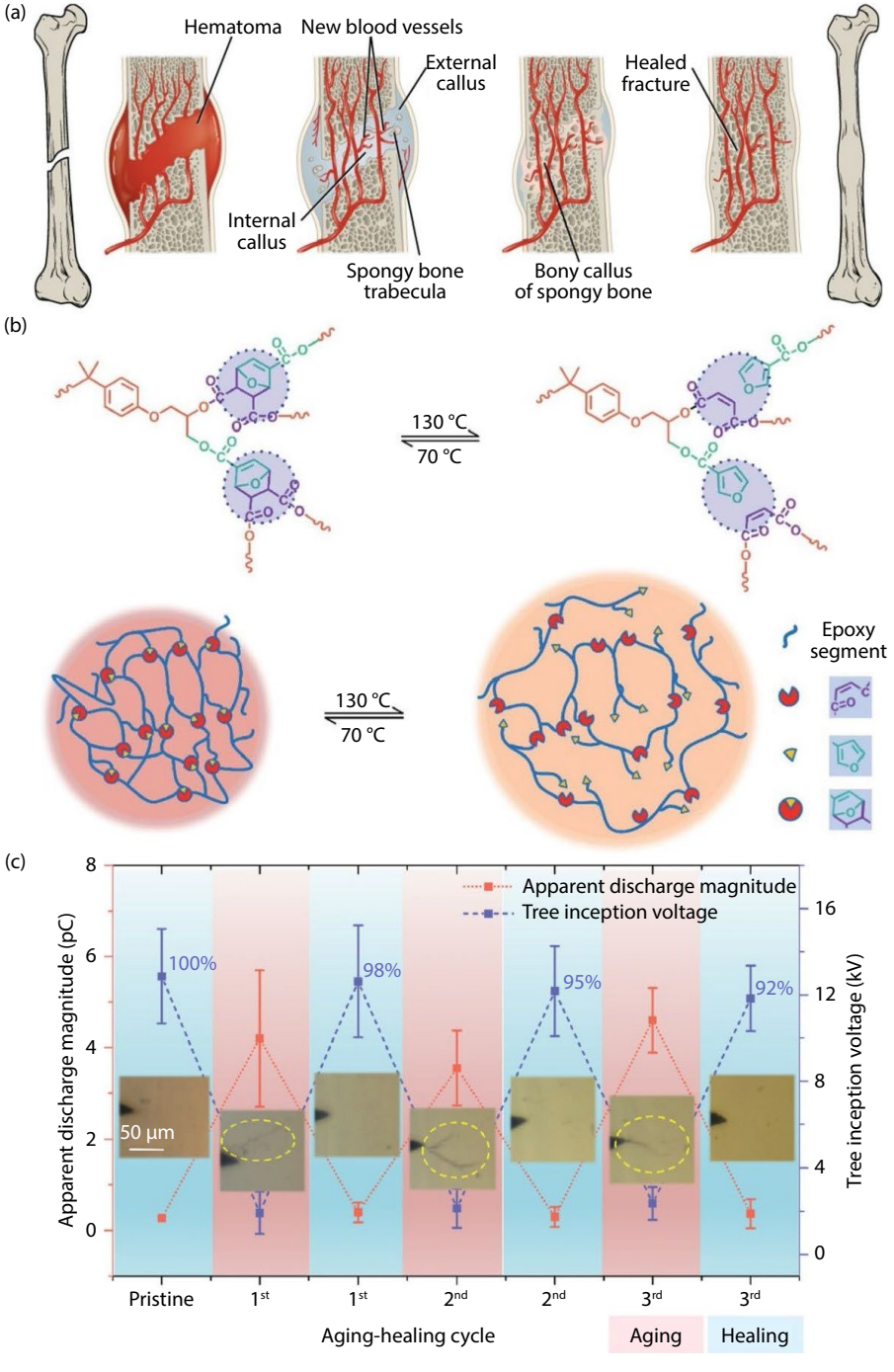

Fig. 20 Inspiration and mechanisms of self-healing by reversible crosslinking networks. (**a**) The healing process of a bone fracture. Spongy bone is first formed at the fracture, and eventually replaced by compact bone (reprinted with permission from ref. [244], © 2021 Rice University). (**b**) Schematic of partially reversible crosslinking network. The polymer network may undergo the conversion between fully crosslinked state and partially crosslinked state under different temperatures (reprinted with permission from ref. [56], © 2021 The Royal Society of Chemistry). (**c**) Insulating properties (apparent partial discharge magnitude and tree inception voltage) and optical images of partially reversible crosslinking epoxy in aging-healing cycles (reprinted with permission from ref. [56], © 2021 The Royal Society of Chemistry).

tiously reporting, significantly responding, and precisely diagnosing are expected to be fabricated. A wide range of materials, mechanisms, and methods of stimuli-responsive polymers, optical chemosensors, and bio-inspired materials can be utilized to design self-reporting dielectrics. Self-healing dielectrics employing more facile, reliable, and repeatable methods need to be manufactured. The materials are preferred to autonomously repair damage as soon as possible without extra treatment, while the properties of the healed region should return to the original level with a highly repeatable healing process.

To fulfill the commercialization of smart dielectrics and its utilization in power apparatus, some obstacles need to be overcome. The stability and endurance of functional additives are crucial. The functional additives, such as ZnO microvaristors, spiropyran chromophores, micro-encapsulated healing agents, etc., are substances that are physically or chemically incorporated into the polymeric matrices to impart materials autonomous functions. The additives are commonly sensitive to harsh environments,

such as overheating, UV irradiation, mechanical stress, acid rain, ozone, free radicals, etc. Hence, their resistance to aging and fatigue in complicated conditions is vital to maintaining the autonomous functions of the smart dielectrics. In addition, incompatible or excessive additives may lead to a performance loss of the matrix, which hampers the implementation of the smart materials in super- or ultra-high voltage engineering. To solve this problem, on one hand, advanced additives with higher performance and better compatibility are required to be developed. The additives should be dispersed into the polymeric matrix more easily and uniformly, contain less reactive agents that may cause material deterioration, as well as have superior performances such as higher resistivity, toughness, elasticity, and thermal conductivity. On the other hand, the smart dielectrics should be more reasonably designed and fabricated to reduce the content of the additives and eliminate defects that are introduced into the polymeric matrix during processing. Furthermore, for practical utilization in the commercial sector, the price of smart dielectrics must be competitive. Therefore, raw material costs should be lowered and synthesis procedures should be simplified. Considering the impact on organisms and the environment, toxicants and pollutants are supposed to be avoided.

The ultimate goal for smart dielectrics is universality and versatility. The autonomous functions apply to a wide range of voltage levels, scenarios, and damage scales. The functional additives are compatible with diverse polymeric matrices, whether it is glassy or rubbery, thermoplastic, or thermoset. Self-adaptive, self-reporting, and self-healing capabilities are organically integrated into identical dielectrics to perform autonomous lifecycle control.

Acknowledgements

This work was financially supported by the National Key R&D Program of China (No. 2018YFE0200100) and the National Natural Science Foundation of China (Nos. U1766221 and 51921005).

Article history

Received: 30 December 2021; Revised: 25 February 2022; Accepted: 7 March 2022

Additional information

Declaration of competing interest

The authors have no competing interests to declare that are relevant to the content of this article.

References

[1] Tanaka, T. (2005). Dielectric nanocomposites with insulating properties. *IEEE Transactions on Dielectrics and Electrical Insulation*, 12: 914–928.

[2] Kozako, M., Fuse, N., Ohki, Y., Okamoto, T., Tanaka, T. (2004). Surface degradation of polyamide nanocomposites caused by partial discharges using IEC (b) electrodes. *IEEE Transactions on Dielectrics and Electrical Insulation*, 11: 833–839.

[3] Imai, T., Sawa, F., Nakano, T., Ozaki, T., Shimizu, T., Kozako, M., Tanaka, T. (2006). Effects of nano- and micro-filler mixture on electrical insulation properties of epoxy based composites. *IEEE Transactions on Dielectrics and Electrical Insulation*, 13: 319–326.

[4] Montanari, G. C., Fabiani, D., Palmieri, F., Kaempfer, D., Thomann, R., Mulhaupt, R. (2004). Modification of electrical properties and performance of EVA and PP insulation through nanostructure by organophilic silicates. *IEEE Transactions on Dielectrics and Electrical Insulation*, 11: 754–762.

[5] Jarvid, M., Johansson, A., Kroon, R., Bjuggren, J. M., Wutzel, H., Englund, V., Gubanski, S., Andersson, M. R., Müller, C. (2015). A new application area for fullerenes: Voltage stabilizers for power cable insulation. *Advanced Materials*, 27: 897–902.

[6] Lewis, T. J. (1994). Nanometric dielectrics. *IEEE Transactions on Dielectrics and Electrical Insulation*, 1: 812–825.

[7] Gorur, R. S., Cherney, E. A., Hackam, R., Orbeck, T. (1988). The electrical performance of polymeric insulating materials under accelerated aging in a fog chamber. *IEEE Transactions on Power Delivery*, 3: 1157–1164.

[8] Morshuis, P. H. F. (2005). Degradation of solid dielectrics due to internal partial discharge: Some thoughts on progress made and where to go now. *IEEE Transactions on Dielectrics and Electrical Insulation*, 12: 905–913.

[9] Shimizu, N., Laurent, C. (1998). Electrical tree initiation. *IEEE Transactions on Dielectrics and Electrical Insulation*, 5: 651–659.

[10] Ruxton, G. D., Allen, W. L., Sherratt, T. N., Speed, M. P. (2018). Avoiding Attack: The Evolutionary Ecology of Crypsis, Aposematism, and Mimicry. Oxford, UK: Oxford University Press.

[11] Leonhardt, U. (2009). Towards invisibility in the visible. *Nature Materials*, 8: 537–538.

[12] Stevens, M., Rong, C. P., Todd, P. A. (2013). Colour change and camouflage in the horned ghost crab Ocypode ceratophthalmus. *Biological Journal of the Linnean Society*, 109: 257–270.

[13] Egan, J., Sharman, R. J., Scott-Brown, K. C., Lovell, P. G. (2016). Edge enhancement improves disruptive camouflage by emphasising false edges and creating pictorial relief. *Scientific Reports*, 6: 38274.

[14] Woodcock, J., Witter, J., Dionne, R. A. (2007). Stimulating the development of mechanism-based, individualized pain therapies. *Nature Reviews Drug Discovery*, 6: 703–710.

[15] Fields, H. (2004). State-dependent opioid control of pain. *Nature Reviews Neuroscience*, 5: 565–575.

[16] Dekoninck, S., Blanpain, C. (2019). Stem cell dynamics, migration and plasticity during wound healing. *Nature Cell Biology*, 21: 18–24.

[17] Witte, M. B., Barbul, A. (1997). General principles of wound healing. *Surgical Clinics of North America*, 77: 509–528.

[18] Stuart-Fox, D., Moussalli, A. (2008). Selection for social signalling drives the evolution of chameleon colour change. *PLoS Biology*, 6: e25.

[19] Teyssier, J., Saenko, S. V., van der Marel, D., Milinkovitch, M. C. (2015). Photonic crystals cause active colour change in chameleons. *Nature Communications*, 6: 6368.

[20] Tracey, W. D. Jr. (2017). Nociception. *Current Biology*, 27: R129–R133.

[21] Rabiller, L., Labit, E., Guissard, C., Gilardi, S., Guiard, B. P., Moulédous, L., Silva, M., Mithieux, G., Pénicaud, L., Lorsignol, A., et al. (2021). Pain sensing neurons promote tissue regeneration in adult mice. *Npj Regenerative Medicine*, 6: 63.

[22] Bloch, R. (1941). Wound healing in higher plants. *The Botanical Review*, 7: 110–146.

[23] Marsell, R., Einhorn, T. A. (2011). The biology of fracture healing. *Injury*, 42: 551–555.

[24] Liu, Z. H., Zhang, F. X., Yu, J., Gao, K. L., Ma, W. M. (2018). Research on key technologies in ±1100 kV ultra-high voltage DC transmission. *High Voltage*, 3: 279–288.

[25] Zeng, F. Z., Chen, X. H., Xiao, G., Li, H., Xia, S., Wang, J. F. (2020). A bioinspired ultratough multifunctional mica-based nanopaper with 3D aramid nanofiber framework as an electrical insulating material. *ACS Nano*, 14: 611–619.

[26] Zhao, X. L., Yang, X., Gao, L., Li, Q., Hu, J., He, J. L. (2017). Tuning the potential distribution of AC cable terminals by stress

cone of nonlinear conductivity material. *IEEE Transactions on Dielectrics and Electrical Insulation*, 24: 2686–2693.
[27] Tanaka, T., Okamoto, T., Nakanishi, K., Miyamoto, T. (1993). Aging and related phenomena in modern electric power systems. *IEEE Transactions on Electrical Insulation*, 28: 826–844.
[28] Cherney, E. A. (2013). Nanodielectrics applications-today and tomorrow. *IEEE Electrical Insulation Magazine*, 29: 59–65.
[29] Bamji, S. S., Bulinski, A. T., Chen, Y., Densley, R. J. (1992). Threshold voltage for electrical tree inception in underground HV transmission cables. *IEEE Transactions on Electrical Insulation*, 27: 402–404.
[30] Yoshida, K., Kozako, M., Ishibe, S., Hikita, M., Kamei, N. (2017). Evaluation on applicability to electrical insulating material of hydrocarbon-based thermosetting resin. *Electronics and Communications in Japan*, 100: 83–90.
[31] Ying, Q. L., Wei, D., Gao, X. Q., Liu, Y. G., Chen, P. (2000). Development of high voltage XLPE power cable system in China. In: Proceedings of the 6th International Conference on Properties and Applications of Dielectric Materials (Cat. No. 00CH36347), Xi'an, China.
[32] Roberts, A. (1995). Stress grading for high voltage motor and generator coils. *IEEE Electrical Insulation Magazine*, 11: 26–31.
[33] He, J. L., Xie, J. C., Hu, J. (2014). Progress of nonlinear polymer composites for improving nonuniform electrical fields. *High Voltage Engineering*, 40: 637–647.
[34] Zhao, X. L., Hu, J., Yuan, Z. K., He, J. L. (2021). Design of adaptive bushing based on field grading materials. *High Voltage*, 6: 625–636.
[35] Oesterheld, J., von Olshausen, R., Poehler, S. (1992). Optimized design of accessories for 245 kV and 420 kV XLPE cables. In: Proceedings of the 1992 International Conference on Large High Voltage Electric Systems, 21–202.
[36] Nelson, P. N., Hervig, H. C. (1984). High dielectric constant materials for primary voltage cable terminations. *IEEE Transactions on Power Apparatus and Systems*, PAS-103: 3211–3216.
[37] Christen, T., Donzel, L., Greuter, F. (2010). Nonlinear resistive electric field grading Part 1: Theory and simulation. *IEEE Electrical Insulation Magazine*, 26: 47–59.
[38] Dissado, L. A., Mazzanti, G., Montanari, G. C. (1997). The role of trapped space charges in the electrical aging of insulating materials. *IEEE Transactions on Dielectrics and Electrical Insulation*, 4: 496–506.
[39] Dakin, T. W. (1948). Electrical insulation deterioration treated as a chemical rate phenomenon. *Transactions of the American Institute of Electrical Engineers*, 67: 113–122.
[40] Steennis, E. F., Kreuger, F. H. (1990). Water treeing in polyethylene cables. *IEEE Transactions on Electrical Insulation*, 25: 989–1028.
[41] Youn, B. H., Huh, C. S. (2005). Surface degradation of HTV silicone rubber and EPDM used for outdoor insulators under accelerated ultraviolet weathering condition. *IEEE Transactions on Dielectrics and Electrical Insulation*, 12: 1015–1024.
[42] Tanaka, T. (1986). Internal partial discharge and material degradation. *IEEE Transactions on Electrical Insulation*, EI-21: 899–905.
[43] Hill, R. M., Dissado, L. A. (1983). Theoretical basis for the statistics of dielectric breakdown. *Journal of Physics C:Solid State Physics*, 16: 2145–2156.
[44] Saha, T. K. (2003). Review of modern diagnostic techniques for assessing insulation condition in aged transformers. *IEEE Transactions on Dielectrics and Electrical Insulation*, 10: 903–917.
[45] Stone, G. C. (2005). Partial discharge diagnostics and electrical equipment insulation condition assessment. *IEEE Transactions on Dielectrics and Electrical Insulation*, 12: 891–904.
[46] Aggarwal, R. K., Johns, A. T., Jayasinghe, J. A. S. B., Su, W. (2000). An overview of the condition monitoring of overhead lines. *Electric Power Systems Research*, 53: 15–22.
[47] Salvatierra, L. M., Kovalevski, L. I., Dammig Quiña, P. L., Irurzun, I. M., Mola, E. E., Dodd, S. J., Dissado, L. A. (2016). Self-healing during electrical treeing: A feature of the two-phase liquid-solid nature of silicone gels. *IEEE Transactions on Dielectrics and Electrical Insulation*, 23: 757–767.
[48] Eichhorn, R. M. (1977). Treeing in solid extruded electrical insulation. *IEEE Transactions on Electrical Insulation*, EI-12: 2–18.
[49] Dissado, L. A., Dodd, S. J., Champion, J. V., Williams, P. I., Alison, J. M. (1997). Propagation of electrical tree structures in solid polymeric insulation. *IEEE Transactions on Dielectrics and Electrical Insulation*, 4: 259–279.
[50] Yang, X., Zhao, X. L., Hu, J., He, J. L. (2018). Grading electric field in high voltage insulation using composite materials. *IEEE Electrical Insulation Magazine*, 34: 15–25.
[51] Zhao, X. L., Yang, X., Li, Q., He, J. L., Hu, J. (2017). Synergistic effect of ZnO microspherical varistors and carbon fibers on nonlinear conductivity and mechanical properties of the silicone rubber-based material. *Composites Science and Technology*, 150: 187–193.
[52] Davis, D. A., Hamilton, A., Yang, J., Cremar, L. D., van Gough, D., Potisek, S. L., Ong, M. T., Braun, P. V., Martínez, T. J., White, S. R., et al. (2009). Force-induced activation of covalent bonds in mechanoresponsive polymeric materials. *Nature*, 459: 68–72.
[53] Peng, H., Sun, X., Cai, F., Chen, X., Zhu, Y., Liao, G., Chen, D., Li, Q., Lu, Y., Zhu, Y., et al. (2009). Electrochromatic carbon nanotube/polydiacetylene nanocomposite fibres. *Nature Nanotechnology*, 4: 738–741.
[54] Yang, Y., He, J., Li, Q., Gao, L., Hu, J., Zeng, R., Qin, J., Wang, S. X., Wang, Q. (2019). Self-healing of electrical damage in polymers using superparamagnetic nanoparticles. *Nature Nanotechnology*, 14: 151–155.
[55] Gao, L., Yang, Y., Xie, J. Y., Zhang, S., Hu, J., Zeng, R., He, J. L., Li, Q., Wang, Q. (2020). Autonomous self-healing of electrical degradation in dielectric polymers using *in situ* electroluminescence. *Matter*, 2: 451–463.
[56] Xie, J. Y., Yang, M. C., Liang, J. J., Hu, J., Li, Q., He, J. L. (2021). Self-healing of internal damage in mechanically robust polymers utilizing a reversibly convertible molecular network. *Journal of Materials Chemistry A*, 9: 15975–15984.
[57] Patrick, J. F., Robb, M. J., Sottos, N. R., Moore, J. S., White, S. R. (2016). Polymers with autonomous life-cycle control. *Nature*, 540: 363–370.
[58] Christen, T., Donzel, L., Greuter, F. (2010). Nonlinear resistive electric field grading Part 1: Theory and simulation. *IEEE Electrical Insulation Magazine*, 26: 47–59.
[59] Donzel, L., Greuter, F., Christen, T. (2011). Nonlinear resistive electric field grading Part 2: Materials and applications. *IEEE Electrical Insulation Magazine*, 27: 18–29.
[60] Qi, X., Zheng, Z., Boggs, S. (2004). Engineering with nonlinear dielectrics. *IEEE Electrical Insulation Magazine*, 20: 27–34.
[61] Auckland, D. W., Su, W. B., Varlow, B. R. (1995). Smart insulation for tree resistance and surge absorption. In: Proceedings of the 1995 Conference on Electrical Insulation and Dielectric Phenomena, Virginia Beach, VA, USA.
[62] Virsberg, L. G., Ware, P. H. (1967). A new termination for underground distribution. *IEEE Transactions on Power Apparatus and Systems*, PAS-86: 1129–1135.
[63] Abd-Rahman, R., Haddad, A., Harid, N., Griffiths, H. (2012). Stress control on polymeric outdoor insulators using Zinc oxide microvaristor composites. *IEEE Transactions on Dielectrics and Electrical Insulation*, 19: 705–713.
[64] Jeroense, M., Saltzer, M., Ghorbani, H. (2014). Technical challenges linked to HVDC cable development. *Revue de l'electricite et de l'electronique*, 4: 3–10.
[65] Eigner, A., Semino, S. (2013). 50 years of electrical-stress control in cable accessories. *IEEE Electrical Insulation Magazine*, 29: 47–55.
[66] Glatz-Reichenbach, J., Meyer, B., Strümpler, R., Kluge-Weiss, P., Greuter, F. (1996). New low-voltage varistor composites. *Journal of Materials Science*, 31: 5941–5944.

[67] Robertson, J., Varlow, B. R. (2003). The AC non linear permittivity characteristics of Barium titanate filled acrylic resin. In: Proceedings of the 7th International Conference on Properties and Applications of Dielectric Materials (Cat. No. 03CH37417), Nagoya, Japan.
[68] Wang, X., Nelson, J. K., Schadler, L. S., Hillborg, H. (2010). Mechanisms leading to nonlinear electrical response of a nano p-SiC/silicone rubber composite. *IEEE Transactions on Dielectrics and Electrical Insulation*, 17: 1687–1696.
[69] Blatter, G., Greuter, F. (1986). Carrier transport through grain boundaries in semiconductors. *Physical Review B, Condensed Matter*, 33: 3952–3966.
[70] Blatter, G., Greuter, F. (1986). Electrical breakdown at semiconductor grain boundaries. *Physical Review B*, 34: 8555–8572.
[71] Yang, X., Hu, J., He, J. L. (2017). Effect of interfacial charge relaxation on conducting behavior of ZnO varistors under time varying electric fields. *Applied Physics Letters*, 110: 182104.
[72] Yang, X., Zhao, X. L., Li, Q., Hu, J., He, J. L. (2018). Nonlinear effective permittivity of field grading composite dielectrics. *Journal of Physics D: Applied Physics*, 51: 075304.
[73] Robertson, J., Varlow, B. R. (2005). Non-linear ferroelectric composite dielectric materials. *IEEE Transactions on Dielectrics and Electrical Insulation*, 12: 779–790.
[74] He, J. L., Hu, J. (2007). Discussions on nonuniformity of energy absorption capabilities of ZnO varistors. *IEEE Transactions on Power Delivery*, 22: 1523–1532.
[75] Long, W. C., Hu, J., Liu, J., He, J. L. (2010). Effects of cobalt doping on the electrical characteristics of Al-doped ZnO varistors. *Materials Letters*, 64: 1081–1084.
[76] Wang, Z. P., Nelson, J. K., Hillborg, H., Zhao, S., Schadler, L. S. (2012). Graphene oxide filled nanocomposite with novel electrical and dielectric properties. *Advanced Materials*, 24: 3134–3137.
[77] Lin, H. F., Lu, W., Chen, G. H. (2007). Nonlinear DC conduction behavior in epoxy resin/graphite nanosheets composites. *Physica B:Condensed Matter*, 400: 229–236.
[78] Yang, X., Meng, P. F., Zhao, X. L., Li, Q., Hu, J., He, J. L. (2018). How nonlinear V-I characteristics of single ZnO microvaristor influences the performance of its silicone rubber composite. *IEEE Transactions on Dielectrics and Electrical Insulation*, 25: 623–630.
[79] Auckland, D. W., Brown, N. E., Varlow, B. R. (1997). Non-linear conductivity in electrical insulation. In: Proceedings of the IEEE 1997 Annual Report Conference on Electrical Insulation and Dielectric Phenomena, Minneapolis, MN, USA.
[80] Tavernier, K., Auckland, D. W., Varlow, B. R. (1998). Improvement in the electrical performance of electrical insulation by nonlinear fillers. ICSD'98. In: Proceedings of the 1998 IEEE 6th International Conference on Conduction and Breakdown in Solid Dielectrics (Cat. No. 98CH36132), Vasteras, Sweden.
[81] Matsuzaki, H., Nakano, T., Ando, H. (2012). Effects of second particles on nonlinear resistance properties of microvaristor-filled composites. In: Proceedings of the 2012 Annual Report Conference on Electrical Insulation and Dielectric Phenomena, Montreal, QC, Canada.
[82] Yang, X., Hu, J., Chen, S., He, J. (2016). Understanding the percolation characteristics of nonlinear composite dielectrics. *Scientific Reports*, 6: 30597.
[83] Nettelblad, B., Rtensson, E. M., Nneby, C., Fvert, U. G., Gustafsson, A. (2003). Two percolation thresholds due to geometrical effects: experimental and simulated results. *Journal of Physics D: Applied Physics*, 36: 399–405.
[84] Martensson, E., Nettelbled, B., Gafvert, U., Palmqvist, L. (1998). Electrical properties of field grading materials with silicon carbide and carbon black. ICSD'98. In: Proceedings of the 1998 IEEE 6th International Conference on Conduction and Breakdown in Solid Dielectrics (Cat. No. 98CH36132), Vasteras, Sweden.
[85] Mashkouri, S., Ghafouri, M., Arsalani, N., Bidadi, H., Mostafavi, H. (2017). Mechanochemical green synthesis of exfoliated graphite at room temperature and investigation of its nonlinear properties based zinc oxide composite varistors. *Journal of Materials Science: Materials in Electronics*, 28: 4839–4846.
[86] Ishibe, S., Mori, M., Kozako, M., Hikita, M. (2014). A new concept varistor with epoxy/microvaristor composite. *IEEE Transactions on Power Delivery*, 29: 677–682.
[87] Mori, M., Komesu, D., Ishibe, S., Kozako, M., Hikita, M. (2014). Study on the formation of microvaristor chains in composite varistors and their electrical characteristics. In: Proceedings of the 2014 IEEE Electrical Insulation Conference, Philadelphia, PA, USA.
[88] Du, B. X., Li, Z. L., Yang, Z. R. (2016). Field-dependent conductivity and space charge behavior of silicone rubber/SiC composites. *IEEE Transactions on Dielectrics and Electrical Insulation*, 23: 3108–3116.
[89] Wang, X., Herth, S., Hugener, T., Siegel, R. W., Nelson, J. K., Schadler, L. S., Hillborg, H., Auletta, T. (2006). Nonlinear electrical behavior of treated ZnO-EPDM nanocomposites. In: Proceedings of the 2006 IEEE Conference on Electrical Insulation and Dielectric Phenomena, Kansas City, MO, USA.
[90] Chen, T., Wang, M. H., Zhang, H. P., Zhao, Z. Y., Liu, T. T. (2016). Novel synthesis of monodisperse ZnO-based core/shell ceramic powders and applications in low-voltage varistors. *Materials & Design*, 96: 329–334.
[91] Nan, C. W., Shen, Y., Ma, J. (2010). Physical properties of composites near percolation. *Annual Review of Materials Research*, 40: 131–151.
[92] Yuan, Z. K., Hu, J., Huang, Z. W., Sun, G., Sun, Y., He, J. L. (2022). Non-linearly conductive ZnO microvaristors/epoxy resin composite prepared by wet winding with polyester fibre cloth. *High Voltage*, 7: 32–40.
[93] Wang, Z., Nelson, J. K., Hillborg, H., Zhao, S., Schadler, L. S. (2012). Nonlinear conductivity and dielectric response of graphene oxide filled silicone rubber nanocomposites. In: Proceedings of the 2012 Annual Report Conference on Electrical Insulation and Dielectric Phenomena, Montreal, QC, Canada.
[94] Mårtensson, E., Gäfvert, U., Lindefelt, U. (2001). Direct current conduction in SiC powders. *Journal of Applied Physics*, 90: 2862–2869.
[95] Kelen, A. (1967). On the theory of non-linear resistive field grading coatings on insulating surfaces. *Elteknik*, 6: 109–112.
[96] Kimura, K., Tsukiji, M., Tani, T., Hirabayashi, S. (1984). Suppression of local heating on a silicon carbide layer by means of divided potentials. *IEEE Transactions on Electrical Insulation*, EI-19: 294–302.
[97] Umemoto, T., Otake, Y., Yoshimura, M., Nada, T., Miyatake, R. (2020). Optimization of double-layer stress grading system for high voltage rotating electrical machines by electric field and thermal coupled analysis. *IEEE Transactions on Dielectrics and Electrical Insulation*, 27: 971–979.
[98] Li, C. Y., Lin, C. J., Hu, J., Liu, W. D., Li, Q., Zhang, B., He, S., Yang, Y., Liu, F., He, J. L. (2018). Novel HVDC spacers by adaptively controlling surface charges–Part I: Charge transport and control strategy. *IEEE Transactions on Dielectrics and Electrical Insulation*, 25: 1238–1247.
[99] Li, C. Y., Lin, C. J., Yang, Y., Zhang, B., Liu, W. D., Li, Q., Hu, J., He, S., Liu, X. L., He, J. L. (2018). Novel HVDC spacers by adaptively controlling surface charges–Part II: Experiment. *IEEE Transactions on Dielectrics and Electrical Insulation*, 25: 1248–1258.
[100] Lin, C. J., Li, Q., Li, C. Y., Zhang, B., Liu, W. D., Yang, Y., Liu, F., Liu, X. L., Hu, J., He, J. L. (2018). Novel HVDC spacers by adaptively controlling surface charges–Part III: Industrialization prospects. *IEEE Transactions on Dielectrics and Electrical Insulation*, 25: 1259–1266.
[101] Donzel, L., Christen, T., Kessler, R., Greuter, F., Gramespacher, H. (2004). Silicone composites for HV applications based on microvaristors. In: Proceedings of the 2004 IEEE International Conference on Solid Dielectrics, Toulouse, France.
[102] Amerpohl, U., Kirchner, M., Böttcher, B., Malin, G. (2002). Dry Type Outdoor Termination with New Stress Control Management.

Paris, France: Cigré.
[103] Wang, N. Y., Cotton, I., Robertson, J., Follmann, S., Evans, K., Newcombe, D. (2010). Partial discharge control in a power electronic module using high permittivity non-linear dielectrics. *IEEE Transactions on Dielectrics and Electrical Insulation*, 17: 1319–1326.
[104] Donzel, L., Schuderer, J. (2012). Nonlinear resistive electric field control for power electronic modules. *IEEE Transactions on Dielectrics and Electrical Insulation*, 19: 955–959.
[105] Rifaie-Graham, O., Apebende, E. A., Bast, L. K., Bruns, N. (2018). Self-reporting fiber-reinforced composites that mimic the ability of biological materials to sense and report damage. *Advanced Materials*, 30: e1705483.
[106] Abot, J. L., Song, Y., Vatsavaya, M. S., Medikonda, S., Kier, Z., Jayasinghe, C., Rooy, N., Shanov, V. N., Schulz, M. J. (2010). Delamination detection with carbon nanotube thread in self-sensing composite materials. *Composites Science and Technology*, 70: 1113–1119.
[107] Tian, Z., Li, Y. C., Zheng, J. J., Wang, S. G. (2019). A state-of-the-art on self-sensing concrete: Materials, fabrication and properties. *Composites Part B: Engineering*, 177: 107437.
[108] Chen, Q., Feng, Y., Zhang, D. Q., Zhang, G. X., Fan, Q. H., Sun, S. N., Zhu, D. B. (2010). Light-triggered self-assembly of a spiropyran-functionalized dendron into nano-/micrometer-sized particles and photoresponsive organogel with switchable fluorescence. *Advanced Functional Materials*, 20: 36–42.
[109] Lu, X., Zhang, Z. D., Sun, X. M., Chen, P. N., Zhang, J., Guo, H., Shao, Z. Z., Peng, H. S. (2016). Flexible and stretchable chromatic fibers with high sensing reversibility. *Chemical Science*, 7: 5113–5117.
[110] Black, A. L., Lenhardt, J. M., Craig, S. L. (2011). From molecular mechanochemistry to stress-responsive materials. *Journal of Materials Chemistry*, 21: 1655–1663.
[111] Ivashenko, O., van Herpt, J. T., Feringa, B. L., Rudolf, P., Browne, W. R. (2013). Electrochemical write and read functionality through oxidative dimerization of spiropyran self-assembled monolayers on gold. *The Journal of Physical Chemistry C*, 117: 18567–18577.
[112] Abdollahi, A., Rad, J. K., Mahdavian, A. R. (2016). Stimuli-responsive cellulose modified by epoxy-functionalized polymer nanoparticles with photochromic and solvatochromic properties. *Carbohydrate Polymers*, 150: 131–138.
[113] Scarmagnani, S., Walsh, Z., Slater, C., Alhashimy, N., Paull, B., Macka, M., Diamond, D. (2008). Polystyrene bead-based system for optical sensing using spiropyran photoswitches. *Journal of Materials Chemistry*, 18: 5063–5071.
[114] Park, M. K., Kim, K. W., Ahn, D. J., Oh, M. K. (2012). Label-free detection of bacterial RNA using polydiacetylene-based biochip. *Biosensors and Bioelectronics*, 35: 44–49.
[115] Caruso, M. M., Davis, D. A., Shen, Q. L., Odom, S. A., Sottos, N. R., White, S. R., Moore, J. S. (2009). Mechanically-induced chemical changes in polymeric materials. *Chemical Reviews*, 109: 5755–5798.
[116] Calvino, C. (2021). Polymer-based mechanochromic composite material using encapsulated systems. *Macromolecular Rapid Communications*, 42: 2000549.
[117] Ma, L. W., Ren, C. H., Wang, J. K., Liu, T., Yang, H., Wang, Y. J., Huang, Y., Zhang, D. W. (2021). Self-reporting coatings for autonomous detection of coating damage and metal corrosion: A review. *Chemical Engineering Journal*, 421: 127854.
[118] Abdollahi, A., Roghani-Mamaqani, H., Razavi, B. (2019). Stimuli-chromism of photoswitches in smart polymers: Recent advances and applications as chemosensors. *Progress in Polymer Science*, 98: 101149.
[119] Qian, X. M., Städler, B. (2019). Recent developments in polydiacetylene-based sensors. *Chemistry of Materials*, 31: 1196–1222.
[120] Samanta, S., Locklin, J. (2008). Formation of photochromic spiropyran polymer brushes via surface-initiated, ring-opening metathesis polymerization: Reversible photocontrol of wetting behavior and solvent dependent morphology changes. *Langmuir*, 24: 9558–9565.
[121] Exarhos, G. J., Risen, W. M. Jr, Baughman, R. H. (1976). Resonance Raman study of the thermochromic phase transition of a polydiacetylene. *Journal of the American Chemical Society*, 98: 481–487.
[122] Calvino, C., Neumann, L., Weder, C., Schrettl, S. (2017). Approaches to polymeric mechanochromic materials. *Journal of Polymer Science Part A: Polymer Chemistry*, 55: 640–652.
[123] Sheng, L., Li, M., Zhu, S., Li, H., Xi, G., Li, Y. G., Wang, Y., Li, Q., Liang, S., Zhong, K., et al. (2014). Hydrochromic molecular switches for water-jet rewritable paper. *Nature Communications*, 5: 3044.
[124] Chanakul, A., Traiphol, N., Faisadcha, K., Traiphol, R. (2014). Dual colorimetric response of polydiacetylene/zinc oxide nanocomposites to low and high pH. *Journal of Colloid and Interface Science*, 418: 43–51.
[125] Wagner, K., Byrne, R., Zanoni, M., Gambhir, S., Dennany, L., Breukers, R., Higgins, M., Wagner, P., Diamond, D., Wallace, G. G., et al. (2011). A multiswitchable poly(terthiophene) bearing a spiropyran functionality: Understanding photo- and electrochemical control. *Journal of the American Chemical Society*, 133: 5453–5462.
[126] Gao, R., Cao, D., Guan, Y., Yan, D. P. (2016). Fast and reversible humidity-responsive luminescent thin films. *Industrial & Engineering Chemistry Research*, 55: 125–132.
[127] Zheng, Y. J., Orbulescu, J., Ji, X. J., Andreopoulos, F. M., Pham, S. M., Leblanc, R. M. (2003). Development of fluorescent film sensors for the detection of divalent copper. *Journal of the American Chemical Society*, 125: 2680–2686.
[128] Ma, H. Y., Gao, R., Yan, D. P., Zhao, J. W., Wei, M. (2013). Organic–inorganic hybrid fluorescent ultrathin films and their sensor application for nitroaromatic explosives. *Journal of Materials Chemistry C*, 1: 4128–4137.
[129] Lee, S., Park, J. W. (2017). Luminescent oxygen sensors with highly improved sensitivity based on a porous sensing film with increased oxygen accessibility and photoluminescence. *Sensors and Actuators B: Chemical*, 249: 364–377.
[130] Di, S. R. (2015). Fibre optic sensors for structural health monitoring of aircraft composite structures: Recent advances and applications. *Sensors*, 15: 18666–18713.
[131] Friedrich, K., Almajid, A. A. (2013). Manufacturing aspects of advanced polymer composites for automotive applications. *Applied Composite Materials*, 20: 107–128.
[132] Rana, S., Subramani, P., Fangueiro, R., Gomes Correia, A. (2016). A review on smart self-sensing composite materials for civil engineering applications. *AIMS Materials Science*, 3: 357–379.
[133] Yang, R. Z., He, Y. Z., Zhang, H. (2016). Progress and trends in nondestructive testing and evaluation for wind turbine composite blade. *Renewable and Sustainable Energy Reviews*, 60: 1225–1250.
[134] Zhang, Z. J., Wang, L. M., Wang, J., Jiang, X. M., Li, X. H., Hu, Z. J., Ji, Y. L., Wu, X. C., Chen, C. Y. (2012). Mesoporous silica-coated gold nanorods as a light-mediated multifunctional theranostic platform for cancer treatment. *Advanced Materials*, 24: 1418–1423.
[135] Abdollahi, A., Roghani-Mamaqani, H., Salami-Kalajahi, M., Razavi, B., Sahandi-Zangabad, K. (2020). Encryption and optical authentication of confidential cellulosic papers by ecofriendly multicolor photoluminescent inks. *Carbohydrate Polymers*, 245: 116507.
[136] Guo, Z. Q., Song, N. R., Moon, J. H., Kim, M., Jun, E. J., Choi, J., Lee, J. Y., Bielawski, C. W., Sessler, J. L., Yoon, J. (2012). A benzobisimidazolium-based fluorescent and colorimetric chemosensor for CO_2. *Journal of the American Chemical Society*, 134: 17846–17849.
[137] Zhu, M. Q., Zhu, L. Y., Han, J. J., Wu, W. W., Hurst, J. K., Li, A. D. Q. (2006). Spiropyran-based photochromic polymer nanoparticles with optically switchable luminescence. *Journal of the*

American Chemical Society, 128: 4303–4309.
[138] Kundu, P. K., Samanta, D., Leizrowice, R., Margulis, B., Zhao, H., Börner, M., Udayabhaskararao, T., Manna, D., Klajn, R. (2015). Light-controlled self-assembly of non-photoresponsive nanoparticles. *Nature Chemistry*, 7: 646–652.
[139] Li, S., Bai, H. D., Shepherd, R. F., Zhao, H. C. (2019). Bio-inspired design and additive manufacturing of soft materials, machines, robots, and haptic interfaces. *Angewandte Chemie International Edition*, 58: 11182–11204.
[140] Isapour, G., Lattuada, M. (2018). Bioinspired stimuli-responsive color-changing systems. *Advanced Materials*, 30: e1707069.
[141] Barthelat, F. (2007). Biomimetics for next generation materials. *Philosophical Transactions Series A, Mathematical, Physical*, 365: 2907–2919.
[142] Gillies, E. R. (2020). Reflections on the evolution of smart polymers. *Israel Journal of Chemistry*, 60: 75–85.
[143] Gao, R., Fang, X. Y., Yan, D. P. (2019). Recent developments in stimuli-responsive luminescent films. *Journal of Materials Chemistry C*, 7: 3399–3412.
[144] Calvino, C., Weder, C. (2018). Microcapsule-containing self-reporting polymers. *Small*, 14: 1802489.
[145] Sun, X. M., Chen, T., Huang, S. Q., Li, L., Peng, H. S. (2010). Chromatic polydiacetylene with novel sensitivity. *Chemical Society Reviews*, 39: 4244–4257.
[146] Rougeau, L., Picq, D., Rastello, M., Frantz, Y. (2008). New irreversible thermochromic polydiacetylenes. *Tetrahedron* , 64: 9430–9436.
[147] Grogan, C., Florea, L., Koprivica, S., Scarmagnani, S., O'Neill, L., Lyng, F., Pedreschi, F., Benito-Lopez, F., Raiteri, R. (2016). Microcantilever arrays functionalised with spiropyran photoactive moieties as systems to measure photo-induced surface stress changes. *Sensors and Actuators B: Chemical*, 237: 479–486.
[148] Kim, S. H., Suh, H. J., Cui, J. Z., Gal, Y. S., Jin, S. H., Koh, K. (2002). Crystalline-state photochromism and thermochromism of new spiroxazine. *Dyes and Pigments*, 53: 251–256.
[149] Jochum, F. D., Theato, P. (2010). Thermo- and light responsive micellation of azobenzene containing block copolymers. *Chemical Communications*, 46: 6717–6719.
[150] Irie, M. (2000). Diarylethenes for memories and switches. *Chemical Reviews*, 100: 1685–1716.
[151] Klajn, R. (2014). Spiropyran-based dynamic materials. *Chemical Society Reviews*, 43: 148–184.
[152] Lokshin, V., Samat, A., Metelitsa, A. V. (2002). Spirooxazines: synthesis, structure, spectral and photochromic properties. *Russian Chemical Reviews*, 71: 893–916.
[153] Bandara, H. M. D., Burdette, S. C. (2012). Photoisomerization in different classes of azobenzene. *Chemical Society Reviews*, 41: 1809–1825.
[154] Logtenberg, H., van der Velde, J. H. M., de Mendoza, P., Areephong, J., Hjelm, J., Feringa, B. L., Browne, W. R. (2012). Electrochemical switching of conductance with diarylethene-based redox-active polymers. *The Journal of Physical Chemistry C*, 116: 24136–24142.
[155] Sun, B., Hou, Q. X., He, Z. B., Liu, Z. H., Ni, Y. H. (2014). Cellulose nanocrystals (CNC) as carriers for a spirooxazine dye and its effect on photochromic efficiency. *Carbohydrate Polymers*, 111: 419–424.
[156] Wang, G., Tong, X., Zhao, Y. (2004). Preparation of azobenzene-containing amphiphilic diblock copolymers for light-responsive micellar aggregates. *Macromolecules*, 37: 8911–8917.
[157] Gossweiler, G. R., Hewage, G. B., Soriano, G., Wang, Q. M., Welshofer, G. W., Zhao, X. H., Craig, S. L. (2014). Mechanochemical activation of covalent bonds in polymers with full and repeatable macroscopic shape recovery. *ACS Macro Letters*, 3: 216–219.
[158] Bell, N. S., Piech, M. (2006). Photophysical effects between spirobenzopyran-methyl methacrylate-functionalized colloidal particles. *Langmuir*, 22: 1420–1427.
[159] Schenderlein, H., Voss, A., Stark, R. W., Biesalski, M. (2013). Preparation and characterization of light-switchable polymer networks attached to solid substrates. *Langmuir*, 29: 4525–4534.
[160] Beiermann, B. A., Davis, D. A., Kramer, S. L. B., Moore, J. S., Sottos, N. R., White, S. R. (2011). Environmental effects on mechanochemical activation of spiropyran in linear PMMA. *Journal of Materials Chemistry*, 21: 8443–8447.
[161] Grady, M. E., Beiermann, B. A., Moore, J. S., Sottos, N. R. (2014). Shockwave loading of mechanochemically active polymer coatings. *ACS Applied Materials & Interfaces*, 6: 5350–5355.
[162] O'Bryan, G., Wong, B. M., McElhanon, J. R. (2010). Stress sensing in polycaprolactone films via an embedded photochromic compound. *ACS Applied Materials & Interfaces*, 2: 1594–1600.
[163] Lee, C. K., Davis, D. A., White, S. R., Moore, J. S., Sottos, N. R., Braun, P. V. (2010). Force-induced redistribution of a chemical equilibrium. *Journal of the American Chemical Society*, 132: 16107–16111.
[164] Kosuge, T., Imato, K., Goseki, R., Otsuka, H. (2016). Polymer–inorganic composites with dynamic covalent mechanochromophore. *Macromolecules*, 49: 5903–5911.
[165] Kosuge, T., Zhu, X. L., Lau, V. M., Aoki, D., Martinez, T. J., Moore, J. S., Otsuka, H. (2019). Multicolor mechanochromism of a polymer/silica composite with dual distinct mechanophores. *Journal of the American Chemical Society*, 141: 1898–1902.
[166] Zhu, S. Y., Li, M. J., Tang, S. C., Zhang, Y. M., Yang, B., Zhang, S. X. A. (2014). Electrochromic switching and microkinetic behaviour of oxazine derivatives and their applications. *European Journal of Organic Chemistry*, 2014: 1227–1235.
[167] Rosario, R., Gust, D., Hayes, M., Springer, J., Garcia, A. A. (2003). Solvatochromic study of the microenvironment of surface-bound spiropyrans. *Langmuir*, 19: 8801–8806.
[168] Florea, L., McKeon, A., Diamond, D., Benito-Lopez, F. (2013). Spiropyran polymeric microcapillary coatings for photodetection of solvent polarity. *Langmuir*, 29: 2790–2797.
[169] Abdollahi, A., Mouraki, A., Sharifian, M. H., Mahdavian, A. R. (2018). Photochromic properties of stimuli-responsive cellulosic papers modified by spiropyran-acrylic copolymer in reusable pH-sensors. *Carbohydrate Polymers*, 200: 583–594.
[170] Fries, K, Samanta, S, Orski, S, Locklin, J. (2008). Reversible colorimetric ion sensors based on surface initiated polymerization of photochromic polymers. *Chemical Communications*: 6288–6290.
[171] Shiraishi, Y., Adachi, K., Itoh, M., Hirai, T. (2009). Spiropyran as a selective, sensitive, and reproducible cyanide anion receptor. *Organic Letters*, 11: 3482–3485.
[172] Charych, D. H., Nagy, J. O., Spevak, W., Bednarski, M. D. (1993). Direct colorimetric detection of a receptor-ligand interaction by a polymerized bilayer assembly. *Science*, 261: 585–588.
[173] Wang, H., Han, S. H., Hu, Y. F., Qi, Z. M., Hu, C. S. (2017). Polydiacetylene-based periodic mesoporous organosilicas with colorimetric reversibility under multiple stimuli. *Colloids and Surfaces A:Physicochemical and Engineering Aspects*, 517: 84–95.
[174] Kamphan, A., Khanantong, C., Traiphol, N., Traiphol, R. (2017). Structural-thermochromic relationship of polydiacetylene (PDA)/polyvinylpyrrolidone (PVP) nanocomposites: Effects of PDA side chain length and PVP molecular weight. *Journal of Industrial and Engineering Chemistry*, 46: 130–138.
[175] Shin, M. J., Kim, J. D. (2016). Reversible chromatic response of polydiacetylene derivative vesicles in D_2O solvent. *Langmuir*, 32: 882–888.
[176] Van den Heuvel, M., Löwik, D. W. P. M., van Hest, J. C. M. (2010). Effect of the diacetylene position on the chromatic properties of polydiacetylenes from self-assembled peptide amphiphiles. *Biomacromolecules*, 11: 1676–1683.
[177] Peng, J. S., Cheng, Y. R., Tomsia, A. P., Jiang, L., Cheng, Q. F. (2017). Thermochromic artificial nacre based on montmorillonite. *ACS Applied Materials & Interfaces*, 9: 24993–24998.
[178] Park, D. H., Heo, J. M., Jeong, W., Yoo, Y. H., Park, B. J., Kim, J. M. (2018). Smartphone-based VOC sensor using colorimetric polydiacetylenes. *ACS Applied Materials & Interfaces*, 10: 5014–5021.

[179] Park, D. H., Hong, J., Park, I. S., Lee, C. W., Kim, J. M. (2014). A colorimetric hydrocarbon sensor employing a swelling-induced mechanochromic polydiacetylene. *Advanced Functional Materials*, 24: 5186–5193.
[180] Hong, J., Park, D. H., Baek, S., Song, S., Lee, C. W., Kim, J. M. (2015). Polydiacetylene-embedded microbeads for colorimetric and volumetric sensing of hydrocarbons. *ACS Applied Materials & Interfaces*, 7: 8339–8343.
[181] Seo, S., Lee, J., Kwon, M. S., Seo, D., Kim, J. (2015). Stimuli-responsive matrix-assisted colorimetric water indicator of polydiacetylene nanofibers. *ACS Applied Materials & Interfaces*, 7: 20342–20348.
[182] Baek, W., Heo, J. M., Oh, S., Lee, S. H., Kim, J., Joung, J. F., Park, S., Chung, H., Kim, J. M. (2016). Photoinduced reversible phase transition of azobenzene-containing polydiacetylene crystals. *Chemical Communications*, 52: 14059–14062.
[183] Zhang, W., Xu, H. B., Chen, Y., Cheng, S., Fan, L. J. (2013). Polydiacetylene-polymethylmethacrylate/graphene composites as one-shot, visually observable, and semiquantative electrical current sensing materials. *ACS Applied Materials & Interfaces*, 5: 4603–4606.
[184] Song, S., Ha, K., Guk, K., Hwang, S. G., Choi, J. M., Kang, T., Bae, P., Jung, J., Lim, E. K. (2016). Colorimetric detection of influenza A (H1N1) virus by a peptide-functionalized polydiacetylene (PEP-PDA) nanosensor. *RSC Advances*, 6: 48566–48570.
[185] Wang, J. P., Zhao, X. P., Guo, H. L., Zheng, Q. (2004). Preparation of microcapsules containing two-phase core materials. *Langmuir*, 20: 10845–10850.
[186] Pang, J. W. C., Bond, I. P. (2005). 'Bleeding composites'—Damage detection and self-repair using a biomimetic approach. *Composites Part A: Applied Science and Manufacturing*, 36: 183–188.
[187] Patrick, J. F., Hart, K. R., Krull, B. P., Diesendruck, C. E., Moore, J. S., White, S. R., Sottos, N. R. (2014). Continuous self-healing life cycle in vascularized structural composites. *Advanced Materials*, 26: 4302–4308.
[188] White, S. R., Sottos, N. R., Geubelle, P. H., Moore, J. S., Kessler, M. R., Sriram, S. R., Brown, E. N., Viswanathan, S. (2001). Autonomic healing of polymer composites. *Nature*, 409: 794–797.
[189] Vidinejevs, S., Aniskevich, A. N., Gregor, A., Sjöberg, M., Alvarez, G. (2012). Smart polymeric coatings for damage visualization in substrate materials. *Journal of Intelligent Material Systems and Structures*, 23: 1371–1377.
[190] Vidinejevs, S., Strekalova, O., Aniskevich, A., Gaidukov, S. (2013). Development of a composite with an inherent function of visualization of a mechanical action. *Mechanics of Composite Materials*, 49: 77–84.
[191] Li, W. L., Matthews, C. C., Yang, K., Odarczenko, M. T., White, S. R., Sottos, N. R. (2016). Autonomous indication of mechanical damage in polymeric coatings. *Advanced Materials*, 28: 2189–2194.
[192] Di Credico, B., Griffini, G., Levi, M., Turri, S. (2013). Microencapsulation of a UV-responsive photochromic dye by means of novel UV-screening polyurea-based shells for smart coating applications. *ACS Applied Materials & Interfaces*, 5: 6628–6634.
[193] Postiglione, G., Colombo, A., Dragonetti, C., Levi, M., Turri, S., Griffini, G. (2017). Fluorescent probes based on chemically-stable core/shell microcapsules for visual microcrack detection. *Sensors and Actuators B: Chemical*, 248: 35–42.
[194] Odom, S. A., Jackson, A. C., Prokup, A. M., Chayanupatkul, S., Sottos, N. R., White, S. R., Moore, J. S. (2011). Visual indication of mechanical damage using core–shell microcapsules. *ACS Applied Materials & Interfaces*, 3: 4547–4551.
[195] Robb, M. J., Li, W. L., Gergely, R. C. R., Matthews, C. C., White, S. R., Sottos, N. R., Moore, J. S. (2016). A robust damage-reporting strategy for polymeric materials enabled by aggregation-induced emission. *ACS Central Science*, 2: 598–603.
[196] Lavrenova, A., Farkas, J., Weder, C., Simon, Y. C. (2015). Visualization of polymer deformation using microcapsules filled with charge-transfer complex precursors. *ACS Applied Materials & Interfaces*, 7: 21828–21834.
[197] Chen, Y. X., Li, W., Luo, J., Liu, R., Sun, G. Q., Liu, X. Y. (2021). Robust damage-reporting strategy enabled by dual-compartment microcapsules. *ACS Applied Materials & Interfaces*, 13: 14518–14529.
[198] Wu, D. Y., Meure, S., Solomon, D. (2008). Self-healing polymeric materials: A review of recent developments. *Progress in Polymer Science*, 33: 479–522.
[199] Wang, S., Urban, M. W. (2020). Self-healing polymers. *Nature Reviews Materials*, 5: 562–583.
[200] Ieda, M. (1980). Dielectric breakdown process of polymers. *IEEE Transactions on Electrical Insulation*, EI-15: 206–224.
[201] Yang, Y., Dang, Z. M., Li, Q., He, J. L. (2020). Self-healing of electrical damage in polymers. *Advanced Science*, 7: 2002131.
[202] Tao, W. B., Song, S. Y., Bai, R., Wei, X. J., Zhou, K., Li, T. H., Huang, M. (2016). The self-healing phenomenon of non-conducting electrical trees in XLPE cables. In: Proceedings of the 2016 IEEE International Conference on High Voltage Engineering and Application, Chengdu, China.
[203] Rudi, K., Andrew, D. H., Managam, R., Nawawi, Z., Hozumi, N., Nagao, M. (2012). The self-healing property of silicone rubber after degraded by treeing. In: Proceedings of the 2012 IEEE International Conference on Condition Monitoring and Diagnosis, Bali, Indonesia.
[204] Rosensweig, R. E. (2002). Heating magnetic fluid with alternating magnetic field. *Journal of Magnetism and Magnetic Materials*, 252: 370–374.
[205] Fortin, J. P., Wilhelm, C., Servais, J., Ménager, C., Bacri, J. C., Gazeau, F. (2007). Size-sorted anionic iron oxide nanomagnets as colloidal mediators for magnetic hyperthermia. *Journal of the American Chemical Society*, 129: 2628–2635.
[206] Corten, C. C., Urban, M. W. (2009). Repairing polymers using oscillating magnetic field. *Advanced Materials*, 21: 5011–5015.
[207] Ahmed, A. S., Ramanujan, R. V. (2015). Curie temperature controlled self-healing magnet–polymer composites. *Journal of Materials Research*, 30: 946–958.
[208] Yoonessi, M., Lerch, B. A., Peck, J. A., Rogers, R. B., Solá-Lopez, F. J., Meador, M. A. (2015). Self-healing of core-shell magnetic polystyrene nanocomposites. *ACS Applied Materials & Interfaces*, 7: 16932–16937.
[209] Jeoffroy, E., Koulialias, D., Yoon, S., Partl, M. N., Studart, A. R. (2016). Iron oxide nanoparticles for magnetically-triggered healing of bituminous materials. *Construction and Building Materials*, 112: 497–505.
[210] Wool, R. P. (2008). Self-healing materials: A review. *Soft Matter*, 4: 400.
[211] Yang, Y., Gao, L., Xie, J. Y., Zhou, Y., Hu, J., Li, Q., He, J. L. (2020). Defect-targeted self-healing of multiscale damage in polymers. *Nanoscale*, 12: 3605–3613.
[212] Lee, J. Y., Zhang, Q. L., Emrick, T., Crosby, A. J. (2006). Nanoparticle alignment and repulsion during failure of glassy polymer nanocomposites. *Macromolecules*, 39: 7392–7396.
[213] Gupta, S., Zhang, Q., Emrick, T., Balazs, A. C., Russell, T. P. (2006). Entropy-driven segregation of nanoparticles to cracks in multilayered composite polymer structures. *Nature Materials*, 5: 229–233.
[214] Balazs, A. C., Emrick, T., Russell, T. P. (2006). Nanoparticle polymer composites: Where two small worlds meet. *Science* , 314: 1107–1110.
[215] Hall, J., Hall, M. (2020). Guyton and Hall Textbook of Medical Physiology (14th Edition). Amsterdam: Elsevier.
[216] Lee, J. H., Jang, J. T., Choi, J. S., Moon, S. H., Noh, S. H., Kim, J. W., Kim, J. G., Kim, I. S., Park, K. I., Cheon, J. (2011). Exchange-coupled magnetic nanoparticles for efficient heat induction. *Nature Nanotechnology*, 6: 418–422.
[217] Blaiszik, B. J., Kramer, S. L. B., Olugebefola, S. C., Moore, J. S., Sottos, N. R., White, S. R. (2010). Self-healing polymers and com-

posites. *Annual Review of Materials Research*, 40: 179–211.
[218] Diesendruck, C. E., Sottos, N. R., Moore, J. S., White, S. R. (2015). Biomimetic self-healing. *Angewandte Chemie International Edition*, 54: 10428–10447.
[219] Wang, Y. Y., Li, Y. D., Zhang, Z. X., Zhang, Y. F. (2019). Effect of doping microcapsules on typical electrical performances of self-healing polyethylene insulating composite. *Applied Sciences*, 9: 3039.
[220] Li, Y. Q., Wang, Y. Y., Zhang, Y. F., Yaseen, A., Li, Y. D. (2021). Effect of microcapsules on dielectric properties of self-healing low density polyethylene insulation composites. *IEEE Transactions on Dielectrics and Electrical Insulation*, 28: 924–931.
[221] Zhang, Y. F., Wang, Y. Y., Li, Y. D., Huang, Z. Y., Zheng, R. L., Tan, Y. X. (2021). Self-healing of mechanical damage of polyethylene/microcapsules electrical insulation composite material. *Journal of Materials Science:Materials in Electronics*, 32: 26329–26340.
[222] Li, J. Y., Zhang, L., Ducharme, S. (2007). Electric energy density of dielectric nanocomposites. *Applied Physics Letters*, 90: 132901.
[223] Calame, J. P. (2003). Evolution of Davidson-Cole relaxation behavior in random conductor-insulator composites. *Journal of Applied Physics*, 94: 5945–5957.
[224] Li, J. Y., Huang, C., Zhang, Q. M. (2004). Enhanced electromechanical properties in all-polymer percolative composites. *Applied Physics Letters*, 84: 3124–3126.
[225] Lesaint, C., Risinggård, V., Hølto, J., Sæternes, H. H., Hestad, Ø., Hvidsten, S., Glomm, W. R. (2014). Self-healing high voltage electrical insulation materials. In: Proceedings of the 2014 IEEE Electrical Insulation Conference, Philadelphia, PA, USA.
[226] Di Credico, B., Levi, M., Turri, S. (2013). An efficient method for the output of new self-repairing materials through a reactive isocyanate encapsulation. *European Polymer Journal*, 49: 2467–2476.
[227] Suryanarayana, C., Rao, K. C., Kumar, D. (2008). Preparation and characterization of microcapsules containing linseed oil and its use in self-healing coatings. *Progress in Organic Coatings*, 63: 72–78.
[228] Song, Y. K., Jo, Y. H., Lim, Y. J., Cho, S. Y., Yu, H. C., Ryu, B. C., Lee, S. I., Chung, C. M. (2013). Sunlight-induced self-healing of a microcapsule-type protective coating. *ACS Applied Materials & Interfaces*, 5: 1378–1384.
[229] Gao, L., He, J. L., Hu, J., Wang, C. (2015). Photoresponsive self-healing polymer composite with photoabsorbing hybrid microcapsules. *ACS Applied Materials & Interfaces*, 7: 25546–25552.
[230] Guo, W. C., Jia, Y., Tian, K. S., Xu, Z. P., Jiao, J., Li, R. F., Wu, Y. H., Cao, L., Wang, H. Y. (2016). UV-triggered self-healing of a single robust SiO_2 microcapsule based on cationic polymerization for potential application in aerospace coatings. *ACS Applied Materials & Interfaces*, 8: 21046–21054.
[231] Laurent, C., Massines, F., Mayoux, C. (1997). Optical emission due to space charge effects in electrically stressed polymers. *IEEE Transactions on Dielectrics and Electrical Insulation*, 4: 585–603.
[232] Sima, W. X., Liang, C., Sun, P. T., Yang, M., Zhu, C., Yuan, T., Liu, F. Q., Zhao, M. K., Shao, Q. Q., Yin, Z., et al. (2021). Novel smart insulating materials achieving targeting self-healing of electrical trees: High performance, low cost, and eco-friendliness. *ACS Applied Materials & Interfaces*, 13: 33485–33495.
[233] Zhang, C. Y., Jiang, X. B., Rong, M. Z., Zhang, M. Q. (2014). Free radical polymerization aided self-healing. *Journal of Intelligent Material Systems and Structures*, 25: 31–39.
[234] Dailey, M. M. C., Silvia, A. W., McIntire, P. J., Wilson, G. O., Moore, J. S., White, S. R. (2014). A self-healing biomaterial based on free-radical polymerization. *Journal of Biomedical Materials Research Part A*, 102: 3024–3032.
[235] Xiao, D. S., Yuan, Y. C., Rong, M. Z., Zhang, M. Q. (2009). A facile strategy for preparing self-healing polymer composites by incorporation of cationic catalyst-loaded vegetable fibers. *Advanced Functional Materials*, 19: 2289–2296.
[236] Yin, T., Rong, M. Z., Zhang, M. Q., Yang, G. C. (2007). Self-healing epoxy composites—Preparation and effect of the healant consisting of microencapsulated epoxy and latent curing agent. *Composites Science and Technology*, 67: 201–212.
[237] Yin, T., Zhou, L., Rong, M. Z., Zhang, M. Q. (2008). Self-healing woven glass fabric/epoxy composites with the healant consisting of micro-encapsulated epoxy and latent curing agent. *Smart Materials and Structures*, 17: 015019.
[238] Hart, K. R., Sottos, N. R., White, S. R. (2015). Repeatable self-healing of an epoxy matrix using imidazole initiated polymerization. *Polymer*, 67: 174–184.
[239] Xie, J. Y., Gao, L., Hu, J., Li, Q., He, J. L. (2020). Self-healing of electrical damage in thermoset polymers via anionic polymerization. *Journal of Materials Chemistry C*, 8: 6025–6033.
[240] Thakur, V. K., Kessler, M. R. (2015). Self-healing polymer nanocomposite materials: A review. *Polymer*, 69: 369–383.
[241] Yang, Y., Urban, M. W. (2013). Self-healing polymeric materials. *Chemical Society Reviews*, 42: 7446–7467.
[242] Wool, R. P., O'Connor, K. M. (1981). A theory crack healing in polymers. *Journal of Applied Physics*, 52: 5953–5963.
[243] Oberhausen, B., Kickelbick, G. (2021). Induction heating induced self-healing of nanocomposites based on surface-functionalized cationic iron oxide particles and polyelectrolytes. *Nanoscale Advances*, 3: 5589–5604.
[244] Betts, J. G., Young, K., A., Wise, J. A., Johnson, E., Poe, B., Kruse, D. H., Korol, O., Johnson, J. E., Womble, M., DeSaix, P., et al. (2013). Anatomy and Physiology. Houston, Texas, USA: OpenStax.
[245] Chen, X. X., Dam, M. A., Ono, K., Mal, A., Shen, H. B., Nutt, S. R., Sheran, K., Wudl, F. (2002). A thermally re-mendable cross-linked polymeric material. *Science*, 295: 1698–1702.
[246] Plaisted, T. A., Nemat-Nasser, S. (2007). Quantitative evaluation of fracture, healing and re-healing of a reversibly cross-linked polymer. *Acta Materialia*, 55: 5684–5696.
[247] Postiglione, G., Turri, S., Levi, M. (2015). Effect of the plasticizer on the self-healing properties of a polymer coating based on the thermoreversible Diels–Alder reaction. *Progress in Organic Coatings*, 78: 526–531.
[248] Turkenburg, D. H., Fischer, H. R. (2015). Diels-Alder based, thermo-reversible cross-linked epoxies for use in self-healing composites. *Polymer*, 79: 187–194.